Concentric Catheterization to the Fractional non-Newtonian Hybrid Nano Blood Flow through a Stenosed Aneurysmal Artery

Obaid Ullah Mehmood (obaid.mahmood@yahoo.com)
COMSATS University Islamabad
Sehrish Bibi
COMSATS University Islamabad
Dzuliana F. Jamil
Tun Hussein Onn University of Malaysia
Salah Uddin
Qurtuba University of Science and Information Technology
Rozaini Roslan
Tun Hussein Onn University of Malaysia
Mohd Kamalrulzaman Md Akhir
Universiti Malaysia Perlis

Research Article

Keywords: Hybrid nanofluid, Blood flow, Stenosis, Aneurysm, Concentric Catheterization, Fractional second-grade fluid

Posted Date: April 13th, 2021

DOI: https://doi.org/10.21203/rs.3.rs-384264/v1

Concentric Catheterization to the Fractional non-Newtonian Hybrid Nano Blood Flow through a Stenosed Aneurysmal Artery

Obaid Ullah Mehmood[a,*], Sehrish Bibi[a], Dzuliana F. Jamil[b], Salah Uddin[c], Rozaini Roslan[b,e], Mohd Kamalrulzaman Md Akhir[d,e]

[a]Department of Mathematics, COMSATS University Islamabad, Wah Campus, Wah Cantt. 47040, Pakistan

[b]Faculty of Applied Sciences and Technology, Universiti Tun Hussein Onn Malaysia, Pagoh Campus, 84600 Muar, Johor, Malaysia

[c]Department of Physical and Numerical Sciences, Qurtuba University of Science and Information Technology, Peshawar, 25000, Pakistan.

[d]Institute of Engineering Mathematics, Faculty of Applied and Human Sciences, Universiti Malaysia Perlis, Pauh Putra Campus, 02600 Arau, Perlis, Malaysia.

[e]ANNA Systems LLC, Moscow Region, Dubna, 9 Maya Street, Building 7B, Building 2 Ofce 10.141707, Moscow, Dolgoprudnenskoe Highway, 3, Fiztekhpark, Moscow 141980, Russia

Abstract: The main theme of this paper is to analyze the effects of concentric catheterization to the diseased arterial segment having both stenosis and aneurysm along its boundary. Fractional second grade hybrid nanofluid model is under consideration. Governing equations are formulated and further linearized for both cases of mild stenosis and aneurysm. Precise articulations for various important flow characteristics heat transfer, hemodynamic velocity, wall shear stress and resistance impedance are attained. Graphical portrayals for the impact of the significant parameters on the flow attributes have been devised and talked about. The worldwide conduct of blood has been examined using an instantaneous streamlines pattern. The present concept plans to be of use in medical regime for the drug conveyance system and biomedicines.

Keywords: Hybrid nanofluid; Blood flow; Stenosis; Aneurysm; Concentric Catheterization; Fractional second-grade fluid.

1. Introduction

Arterial stenosis and arterial aneurysm have attained very widespread attention because of their recurrent occurrence in both young grownup and pediatric patients. A normal blood circulation within human body is vital for the provision of nutrients, oxygen and functions like waste dismissal. The excess of certain nutrients like cholesterol and fat can result in blockage or expansion of the arteries that deliver blood from the heart to different parts of the body. Many people die as a result of it. The constriction or limitation of an artery or heart valve disturbing normal blood stream is known as stenosis and the associated disease is known as arteriosclerosis. Arteriosclerosis occurs as the arteries turn out to be thick and solid causing coronary artery infections, myocardial infarction, strokes, angina, and cardiac arrests. On the other hand, aneurysm is the expansion of an artery brought about by frailty in the arterial wall. Blood flow through veins turns out to be more confounded because of improvement of aneurysm. A cracked aneurysm can prompt lethal intricacies like high blood pressure, atherosclerosis, trauma and abnormal blood flow. In this way, it's important to look at the effects of dilatations and stenosis on blood flow in these narrow arteries. Numerous experts have studied the various blood flow streams through regular, aneurysmal and stenotic arteries, as shown by the references [1-9].

Catheterization is now the most standard medical method for diagnosing and treating arterial diseases. Catheter is a dainty, empty cylinder that is injected into the vein. It tends to be utilized to maximize the supply of blood to indispensable organs. Besides, it can every now and again measure the degrees of gases carbon dioxide and oxygen in the circulation system. When a blood vessel is narrowed or blocked, a catheter with a balloon may be used to expand the vein and increase blood flow. The study of blood circulation via stenotic and aneurysmal arteries is gaining prominence, owing to the ever-increasing requirements of science and medicine. Numerous hypothetical examinations have been acquainted with represent the impact of addition of catheter in the presence of stenosis and on the blood stream, as demonstrated by the citations [10-16]

Nanotechnology centers around miniature items and the creation of issue. The nanoparticle organized measurement is 100 nanometers. The innate capacity of nanotechnology permits the transport of prescriptions to various segments of the human body empowering a proficient conveyance of cargo inside tissues and cells. Nanotechnology is acclaimed as having the capacity to build the proficiency of energy utilization and tackle significant medical conditions. Result of nanotechnology is more modest, more practical and entail less energy. Nanotechnology has helped open a scholarly field of science alongside its applications. By intently noticing explicit materials and their designs, new attributes may likewise be found in that capacity materials are changed into nanoparticles, for example, gold and copper nanoparticles. As an outcome, these most recent advances have a critical clinical notoriety in medication. Another realistic form of nanofluids is hybrid nanofluid, which is made of two or more nanomaterials. Adjoining nanoparticles to base liquid upgrade heat transmission qualities of base liquid. A hybrid nanoparticle is an extraordinary compound that blends the compound and actual properties of different segments together and has been endlessly utilized in the production of anticancer medications. Hypothetical examinations that talked about the nanofluid and hybrid nanofluid accessible can be found in the writing [17-29].

For those blood vessels of which widths are under 0.5 mm, blood shows shear-subordinate thickness, limited yield pressure before the stream can start, partition into two stages and a cell-rich focus and a fringe plasma district. These qualities split speculations that are significant for the plan of the overseeing conditions of Newtonian liquid on the grounds that the coronary courses have a distance across under 0.5 mm. appropriately, a non-Newtonian liquid should be utilized for the portrayal of blood development through these arteries. Accordingly, the viscoelastic partial model is picked to depict the blood development through the coronary veins. All things considered, the last model is gotten from the perceived customary worldview by displacing the ordinary time-derivative differential conditions to fractional time-derivative differential equation. In a wide scope of conditions, fractional math has been used to manage distinctive rheological problems. Of the couple of models proposed for physiological liquids, a fractional second-grade liquid model is viewed as significant despite the way that this model limits the fractional time-inferred boundary to a second-grade work ($\alpha = 0$). Further, a set up Naiver Stokes model can be closed from this as an exceptional case by putting the second grade material constant $\lambda_1 = 0$ [30-36].

The main aim of this research is to look at the combined effects of hybrid fractional second-grade fluid model and concentric catheterization in diseased artery having stenosis and aneurysm which has never been done before to the author's knowledge. For mild stenosis and mild aneurysm situations, the constructed problem is simplified to calculate the exact expressions of temperature, hemodynamic velocity, wall shear stress and resistance impedance for the flow. By plotting graphs

and stream lines, the effects of evolving flow parameters are also debated. Finally, in the finishing part, the chief findings of the outcomes are summarized.

2. Problem Formulation

We consider the fractional second-grade hybrid nano blood flow through an annular region bounded by two coaxial tubes. Outer tube contains an axially symmetric mild stenosis and aneurysm while the inner tube represents the catheter. Balloon catheterization is accomplished in the stenotic segment. We deal with the cylindrical coordinate system (r,θ,z) while modelling the flow in such a way that *z*-axis is taken as the axis of the artery and *r*-axis is in the radial direction. Geometries of the outer and the inner walls are defined by

$$R(\bar{z})=\begin{cases}1-\dfrac{\delta}{2b}\left(1+\cos\dfrac{2\pi}{L_j}\left(\bar{z}-\beta_j-\dfrac{L_j}{2}\right)\right), & \beta_j\le\bar{z}\le\beta_j+L_j,\quad j=1,2\\ 1 & (otherwise),\end{cases} \tag{1}$$

$$\chi(\bar{z})=\begin{cases}b\left(e+\sigma Exp(-\pi^2(\bar{z}-z_d-0.5)^2)\right), & \beta_1\le\bar{z}\le\beta_1+L_1,\\ e\ b & (otherwise),\end{cases} \tag{2}$$

where length of the jth irregular stenosed section emanating from the origin is β_j, normal arterial radius is denoted by b, length of jth irregular stenosed section is represented by L_j, and critical height of jth irregular stenosed section is denoted by δ. For stenosis δ is positive and for aneurysm δ is negative. Two specific positions of the critical heights of δ are

$$\bar{z}_1=\beta_1+\frac{L_1}{2},\ \text{and}\quad \bar{z}_2=\beta_2+\frac{L_2}{2}, \tag{3}$$

For the issue viable, we have accepted $L_1=L_2=L_0$ for simplicity. σ is the catheter's maximum height at $\bar{z}=z_d+0.5$, $e\ b$ is the inner radius of the catheter, e is very small and z_d is the axial displacement of the balloon during catheterization.

For fractional second-order derivative we use Caputo's definition

$$D^{\alpha}f(t)=\frac{1}{\Gamma(1-\alpha)}\int_h^t\frac{f^n(t)}{(t-\tau)}\,d\tau,\quad (m-1)<\mathrm{Re}\ (\alpha)<m), \tag{4}$$

where $m\in N$, α is the order of the derivative. And *h* is the initial guess of f. For the derivatives we will use Caputo's derivative condition

$$D^{\alpha}t^{\eta}=\begin{cases}0 & for\ (\eta\le\alpha-1)\\ \dfrac{\Gamma(\eta+1)}{\Gamma(\eta+1-\alpha)}t^{\eta-\alpha} & for\ (\eta>\alpha-1).\end{cases} \tag{5}$$

The physical configuration of the blood flow under consideration is given in figure 1.

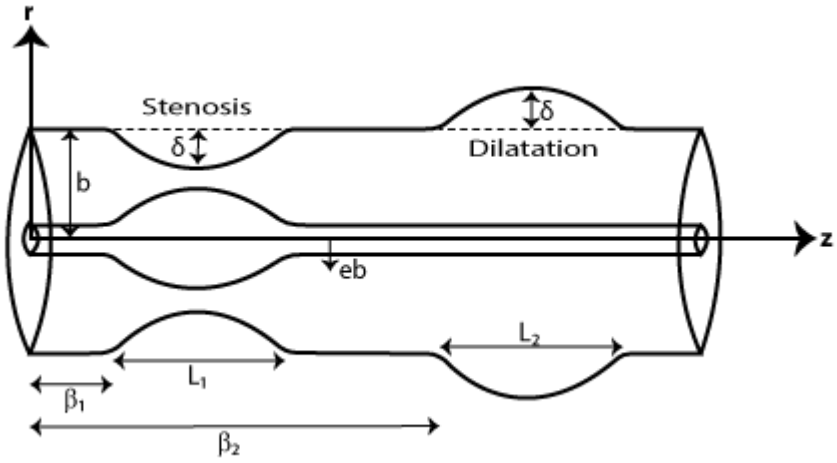

Fig. 1 Configuration of the physical model

The relationship between fractional second-grade and viscoelastic fluids is portrayed by the accompanying [9]:

$$\bar{S}=\mu\left(1+\bar{\lambda}_1\left(\frac{\partial}{\partial\bar{t}}\right)^{\alpha}\right)\dot{\gamma},$$

$$\text{where } \alpha=\begin{cases}0 & \text{Ordinary second-grade fluid}\\ <1 & \text{Fractional second-grade fluid}\end{cases} \tag{6}$$

In the above expression μ is viscosity, $\bar{t}$ is time, $\bar{S}$ is shear stress, $\bar{\lambda}_1$ is material constant, $\dot{\gamma}$ is shear strain rate and α $(0\le\alpha\le1)$ is time-derivative fractional parameter. The fractional second-grade model coincide with ordinary second-grade model if $\alpha=1$ and it reduces to a Navier stoke model if $\bar{\lambda}_1=0$. Along with gravity as a body force, the scalar forms of the governing equations for the axisymmetric flows with the fractional second-grade model for viscoelastic fluid are as follows

$$\frac{\partial\bar{w}}{\partial\bar{z}}+\frac{\bar{u}}{\bar{r}}+\frac{\partial\bar{u}}{\partial\bar{r}}=0, \tag{7}$$

$$\rho_{hnf}\left(\frac{\partial\bar{u}}{\partial\bar{t}}+\bar{w}\frac{\partial\bar{u}}{\partial\bar{z}}+\bar{u}\frac{\partial\bar{u}}{\partial\bar{r}}\right)=-\frac{\partial\bar{p}}{\partial\bar{r}}+\mu_{hnf}\left(1+\bar{\lambda}_1^{\alpha}\left(\frac{\partial}{\partial\bar{t}}\right)^{\alpha}\right)\left[\frac{\partial^2\bar{u}}{\partial\bar{r}^2}+\frac{1}{\bar{r}}\frac{\partial\bar{u}}{\partial\bar{r}}+\frac{\partial^2\bar{u}}{\partial\bar{z}^2}-\frac{\bar{u}^2}{\bar{r}^2}\right], \tag{8}$$

$$\rho_{hnf}\left(\frac{\partial \bar{w}}{\partial \bar{t}}+\bar{w}\frac{\partial \bar{w}}{\partial \bar{z}}+\bar{u}\frac{\partial \bar{w}}{\partial \bar{r}}\right)=-\frac{\partial \bar{p}}{\partial \bar{z}}+\mu_{hnf}\left(1+\bar{\lambda}_1^{\alpha}\left(\frac{\partial}{\partial \bar{t}}\right)^{\alpha}\right)\left[\frac{\partial^2 \bar{w}}{\partial \bar{r}^2}+\frac{1}{\bar{r}}\frac{\partial \bar{w}}{\partial \bar{r}}+\frac{\partial^2 \bar{w}}{\partial \bar{z}^2}\right]+(\rho\gamma)_{hnf}\, g(\bar{T}-\bar{T}_0), \tag{9}$$

$$(\rho c)_{hnf}\left(\frac{\partial \bar{T}}{\partial \bar{t}}+\bar{u}\frac{\partial \bar{T}}{\partial \bar{r}}+\bar{w}\frac{\partial \bar{T}}{\partial \bar{z}}\right)=k_{hnf}\left(\frac{\partial^2 \bar{T}}{\partial \bar{r}^2}+\frac{1}{\bar{r}}\frac{\partial \bar{T}}{\partial \bar{r}}+\frac{\partial^2 \bar{T}}{\partial \bar{z}^2}\right)+Q, \tag{10}$$

where $\bar{r}$ represents radial direction and $\bar{z}$ -axis is taken along the axis of the artery. $\bar{u}$ and $\bar{w}$ are radial and axial velocity components, Q is constant of heat generation or heat absorption, μ_{hnf} , k_{hnf} , ρ_{hnf} , $(\rho c)_{hnf}$ and γ_{hnf} are viscosities, thermal conductivities, densities, heat capacitances and thermal expansions of the hybrid nano particles. T is the fluid temperature.

The appropriate dimensional boundary conditions are

$$\begin{aligned}&\bar{w}=0 \quad \text{at} \quad r=\chi(\bar{z}) \quad \text{and} \quad \bar{w}=0 \quad \text{at} \quad r=R(\bar{z}),\\ &\bar{T}=\bar{T}_0 \quad \text{at} \quad r=\chi(\bar{z}) \quad \text{and} \quad \bar{T}=\bar{T}_0 \quad \text{at} \quad r=R(\bar{z}).\end{aligned} \tag{11}$$

Thermophysical properties of nano blood flow are described as [9]

$$\begin{aligned}&\frac{\mu_{nf}}{\mu_f}=\frac{1}{(1-\phi)^{2.5}},\ (\rho c)_{nf}=(1-\phi)(\rho c)_f+\phi(\rho c)_s,\\ &(\rho\gamma)_{nf}=(1-\phi)(\rho\gamma)_f+\phi(\rho\gamma)_s,\ \rho_{nf}=(1-\phi)\rho_f+\phi\rho_s,\\ &\frac{k_{nf}}{k_f}=\frac{k_s+2k_f-2\phi(-k_f+k_s)}{k_s+2k_f-\phi(-k_f+k_s)}.\end{aligned} \tag{12}$$

Thermophysical properties of Hybrid nano blood flow are described as [9]

$$\begin{aligned}&\frac{\mu_{hnf}}{\mu_f}=\frac{1}{(1-\phi_1)^{2.5}(1-\phi_2)^{2.5}},\\ &\frac{(\rho\gamma)_{hnf}}{(\rho\gamma)_f}=\left((1-\phi_2)\left((1-\phi_1)+\phi_1\frac{(\rho\gamma)_{s1}}{(\rho\gamma)_f}\right)+\phi_2\frac{(\rho\gamma)_{s2}}{(\rho\gamma)_f}\right),\\ &\frac{k_{hnf}}{k_{bf}}=\frac{k_{s2}+(n-1)k_{bf}-(n-1)\phi_2(k_{bf}-k_{s2})}{k_{s2}+(n-1)k_{bf}+\phi_2(k_{bf}-k_{s2})},\\ &\frac{k_{bf}}{k_f}=\frac{k_{s1}+(n-1)k_f-(n-1)\phi_1(k_f-k_{s1})}{k_{s1}+(n-1)k_f+\phi_1(k_f-k_{s1})}.\end{aligned} \tag{13}$$

where μ_f, ρ_f, $(\rho c)_f$, k_f and γ_f are namely viscosity, density , heat capacitance , thermal conductivity and thermal expansion of the base fluid. ρ_s, $(\rho c)_s$, k_s and γ_s are density , heat

capacitance , thermal conductivity and thermal expansion of the nanoparticles and ϕ is the volume friction of nanofluid. Similarly ρ_{s1} and ρ_{s2} , γ_{s1} and γ_{s2} , k_{s1} and k_{s1} are densities , thermal expansions, thermal conductivities of the hybrid nanoparticles respectively. ϕ_1 and ϕ_2 are the volume frictions of nanoparticles. n is the shape factor of nanoparticles.

A distinction between hybrid nanofluid and nanofluid is made. Table 1 provides thermophysical quantitative data for the particular thermal expansion, thermal conductivity and density of blood containing Au and Al_2O_3 nanoparticles. Table 2 shows the shapes of nanoparticles and their related shape factors.

Table 1
Thermophysical properties of hybrid nano particles

Physical properties	Fluid phase (*f*)	nanoparticles phases (*s*)	
		Solid phase (s_1)	Solid phase (s_2)
	Blood	Au	Al_2O_3
$\gamma(kg/m^3)$	0.18	1.42	8.9
$k(W/mk)$	0.492	400	40
$\rho(kg/m^3)$	1063	19300	3970

Table 2
Nano particles shapes factors

Shapes	Platelets	Cylinders	Bricks	Spheres
Shape Factors	5.7	4.9	3.7	3

3. Mild Disease Approximations

We define following variables for the non-dimensionalization

$$r=\frac{\bar{r}}{b},\ w=\frac{\bar{w}}{U},\ z=\frac{\bar{z}}{L_j},\ \ u=\frac{L_j\bar{u}}{U\delta},\ p=\frac{b^2}{UL_j\mu_f}\bar{p},\ t=\frac{U\bar{t}}{L_j},\ \lambda_1=\frac{U\bar{\lambda}_1}{L_j},$$
$$G_r=\frac{(\rho\gamma)_f\, gb^2\bar{T}_0}{\mu_f U},\ \theta=\frac{\bar{T}-\bar{T}_0}{\bar{T}_0}. \tag{14}$$

where U is defined as the velocity averaged over the section of the tube having radius b, temperature is expressed through θ and G_r is the Grashof number. Under the assumptions of mild stenosis and mild aneurysm we apply the following conditions

$$a=\frac{\delta}{b}<<1, \tag{15}$$

$$\Omega = \frac{b}{L_j} \approx 0(1). \tag{16}$$

Equations (7) to (10) in linearized forms after using dimensionless quantities take the forms

$$\frac{\partial p}{\partial r} = 0, \tag{17}$$

$$\frac{\partial p}{\partial z} = \frac{\mu_{hnf}}{\mu_f}\left(1 + \lambda_1{}^{\alpha}\left(\frac{\partial}{\partial t}\right)^{\alpha}\right)\left[\frac{\partial^2 w}{\partial r^2} + \frac{1}{r}\frac{\partial w}{\partial r}\right] + \frac{(\rho\gamma)_{hnf}}{(\rho\gamma)_f} G_r\theta\,, \tag{18}$$

$$\frac{\partial^2 \theta}{\partial r^2} + \frac{1}{r}\frac{\partial \theta}{\partial r} + Q\frac{k_f}{k_{hnf}} = 0\,. \tag{19}$$

The dimensionless boundary conditions are

$$\begin{aligned} &w = 0 \quad \text{at} \quad r = \chi(z) \quad \text{and} \quad w = 0 \quad \text{at} \quad r = R(z), \\ &\theta = 0 \quad \text{at} \quad r = \chi(z) \quad \text{and} \quad \theta = 0 \quad \text{at} \quad r = R(z). \end{aligned} \tag{20}$$

The dimensionless forms of arterial and catheter walls $R(z)$ and $\chi(z)$ are

$$R(z) = \begin{cases} 1 - \dfrac{a}{2}\left(1 + \cos 2\pi\left(z - \varepsilon - \dfrac{1}{2}\right)\right), & \varepsilon \le z \le \varepsilon + 1, \\ 1 & (otherwise), \end{cases} \tag{21}$$

where $\varepsilon = \dfrac{\beta_j}{L_j}$, *and* $j = 1, 2.$

$$\chi(z) = \begin{cases} e + \sigma Exp\left(-\pi^2 L_1{}^2\left(z - \dfrac{z_d + 0.5}{L_1{}^2}\right)^2\right), & \varepsilon_1 \le z \le \varepsilon_1 + 1, \\ e & (otherwise), \end{cases} \tag{22}$$

4. Solution of the Problem

The closed form solutions for temperature and hemodynamic velocity are obtained by solving equations (17) to (19) after applying boundary conditions specified in equation (20) and we obtain

$$\theta(r) = \frac{Q\left((R-\chi)(R+\chi)\,Log[r] + \left(-r^2 + \chi^2\right)Log[R] + (r-R)(r+R)\,Log[\chi]\right)k_f}{4\left(Log[R] - Log[\chi]\right)k_{hnf}}, \tag{23}$$

$$w(r)=\frac{\mu_f}{64c\left(Log[R]-Log[\chi]\right)^2 k_{hnf}\mu_{hnf}\left(\rho\gamma\right)_f}\begin{pmatrix}-16\dfrac{dp}{dz}\left(Log[R]-Log[\chi]\right)\begin{pmatrix}\left(R-\chi\right)\left(R+\chi\right)Log[r]+\\\left(-r^2+\chi^2\right)Log[R]+\\\left(r-R\right)\left(r+R\right)Log[\chi]\end{pmatrix}\\k_{hnf}\left(\rho\gamma\right)_f+G_rQ\mathrm{A}(r)k_f\left(\rho\gamma\right)_{hnf}\end{pmatrix}. \quad (24)$$

where $c=1+\lambda_1{}^{\alpha}\left(\dfrac{\partial}{\partial t}\right)^{\alpha}$ and

$$\mathrm{A}(r)=\left(r^4-4r^2\chi^2+3\chi^4\right)Log[R]^2+\left(R-\chi\right)\left(R+\chi\right)Log[r]\begin{pmatrix}-4\left(R-\chi\right)\left(R+\chi\right)-\left(4r^2-3\left(R^2+\chi^2\right)\right)\\\left(Log[R]-Log[\chi]\right)\end{pmatrix}+$$
$$\left(r-R\right)\left(r+R\right)Log[\chi]\left(-4R^2+4\chi^2+\left(r^2-3R^2\right)Log[\chi]\right)+Log[R]$$
$$\left(4\left(r-\chi\right)\left(R-\chi\right)\left(r+\chi\right)\left(R+\chi\right)+\left(-2r^4+4r^2\left(R^2+\chi^2\right)-3\left(R^4+\chi^4\right)\right)Log[\chi]\right).$$

5. Significant Flow Characteristics

The suitable articulation for volume flow rate in dimensionless form is defines as

$$F(z)=\int_{\chi}^{R} rw\ dr\,. \quad (25)$$

The volume flow rate $F(z)$ can also be written in the form of linear combination of S_1 and S_2 where S_1 and S_2 are given below

$$F(z)=S_1\frac{dp}{dz}+S_2, \quad (26)$$

$$S_1=-\frac{\left(R-\chi\right)\left(R+\chi\right)\left(-R^2+\chi^2+\left(R^2+\chi^2\right)\left(Log[R]-Log[\chi]\right)\right)\mu_f}{16c\left(Log[R]-Log[\chi]\right)\mu_{hnf}}, \quad (27)$$

$$S_2=\frac{G_rQ\left(R-\chi\right)\left(R+\chi\right)\begin{pmatrix}6\left(R^2-\chi^2\right)^2+\begin{pmatrix}-9R^4+9\chi^4+\\4\left(R^4+R^2\chi^2+\chi^4\right)\\\left(Log[R]-Log[\chi]\right)\end{pmatrix}\left(Log[R]-Log[\chi]\right)\end{pmatrix}k_f\mu_f\left(\rho\gamma\right)_{hnf}}{384c\left(Log[R]-Log[\chi]\right)^2 k_{hnf}\mu_{hnf}\left(\rho\gamma\right)_f}, \quad (28)$$

$$\frac{dp}{dz}=\frac{F-S_2}{S_1}\,. \quad (29)$$

Articulations for pressure rise and resistance impedance for non-dimensional arterial segment under consideration is given by

$$\Delta p = \int_0^1 \left(-\frac{dp}{dz} \right) dz\,, \tag{30}$$

$$\lambda = \frac{\Delta p}{F}\,. \tag{31}$$

Expressions for wall shear stress on arterial wall segment and catheter wall segment in dimensionless forms are given as

$$\tau_R = \left(\frac{\partial w}{\partial r} \right)\Big|_{r=R(z)}\,, \tag{32}$$

$$\tau_\chi = \left(\frac{\partial w}{\partial r} \right)\Big|_{r=\chi(z)}\,. \tag{33}$$

Stream function ψ is calculated in the following structure

$$\psi = \frac{\mu_f}{768c\left(Log[R]-Log[\chi]^2\right)k_{hnf}\mu_{hnf}\left(\rho\gamma\right)_f} \left(\begin{array}{l} 48\dfrac{dp}{dz}\left(Log[R]-Log[\chi]\right)\left(\begin{array}{l} 2r^2\left(-R^2+\chi^2\right)Log[r]+ \\ (r-\chi)(r+\chi) \\ \left(\begin{array}{l} R^2-\chi^2+(r-\chi) \\ (r+\chi)Log[R] \end{array} \right)- \\ \left(r^4-2r^2R^2+\chi^4\right)Log[\chi] \end{array} \right) \\ k_{hnf}\left(\rho\gamma\right)_f + G_r Q\mathrm{B}(r)k_f\left(\rho\gamma\right)_{hnf} \end{array} \right) \tag{34}$$

where $c = 1+\lambda_1{}^{\alpha}\left(\dfrac{\partial}{\partial t}\right)^{\alpha}$ and

$$\begin{aligned} \mathrm{B}(r)=&(r-\chi)(r+\chi)\left(12\left(R^2-\chi^2\right)^2+Log[R]\left(-3(R-\chi)(R+\chi)\left(-5r^2+3R^2+6\chi^2\right)+2\left(r^4-5r^2\chi^2+4\chi^4\right)Log[R]\right)\right)- \\ &6r^2(R-\chi)(R+\chi)Log[r]\left(4(R-\chi)(R+\chi)+\left(2r^2-3\left(R^2+\chi^2\right)\right)\left(Log[R]-Log[\chi]\right)\right)- \\ &\left(3(R-\chi)(R+\chi)\left(5r^4+3\chi^2\left(R^2+2\chi^2\right)-r^2\left(11R^2+3\chi^2\right)\right)+2\left(2r^6-8\chi^6-6r^4\left(R^2+\chi^2\right)+9r^2\left(R^4+\chi^4\right)\right)Log[R]\right) \\ &Log[\chi]+2\left(\left(r^3-3rR^2\right)^2-4\chi^6\right)Log[\chi]^2. \end{aligned}$$

6. Graphical Outcomes and Analysis

The determined articulation for temperature and hemodynamic velocity have been acquired for hybrid nano blood stream model. The dynamical features of the wall shear stress, resistance impedance and pressure rise are characterized. Some significant qualities have been explored for different parameters emerging in the solution articulation on the arterial wall segment containing both stenosis and aneurysm in the presence of catheter. Specifically, the effects of the fractional

parameter α, the relaxation time λ_1, Grashof number G_r, heat source Q, nanoparticles shape factor n , nanoparticles volume frictions ϕ_1 and ϕ_2, catheter's maximum height parameter σ, catheter radius parameter e and maximum height a of stenosis and aneurysm. A graphical examination is set to analyze between the stenosis section ($a > 0$) and aneurysm section ($a < 0$). To calculate the numerical closed-form expression for resistance impedance and pressure rise we utilized the numerical integration.

6.1 Temperature

The temperature distribution against the radial coordinate r has been plotted for different values of heat source parameter Q, nanoparticles shape factor n, catheter's radius parameter e and catheter's maximum height parameter σ for stenosis and aneurysm region and for nanofluid and hybrid nanofluid in Fig. 2. In Fig. 2(a) an examination among hybrid nanofluid and nanofluid is likewise made. It is seen that the heat transfer for nanofluid is lower than that of hybrid nanofluid. It is found in Figs. 2(b) and 2(c) that the temperature drops for spherical-shaped hybrid nanoparticles and by increasing e. And temperature in stenosis segment is much lower than that of dilatation segment. From Fig. 2(d) we can see that the temperature decreases by increasing σ in stenosis segment and remains unchanged in dilatation segment. Moreover, it is observed that the temperature in stenosis segment is much lower than that of dilatation segment.

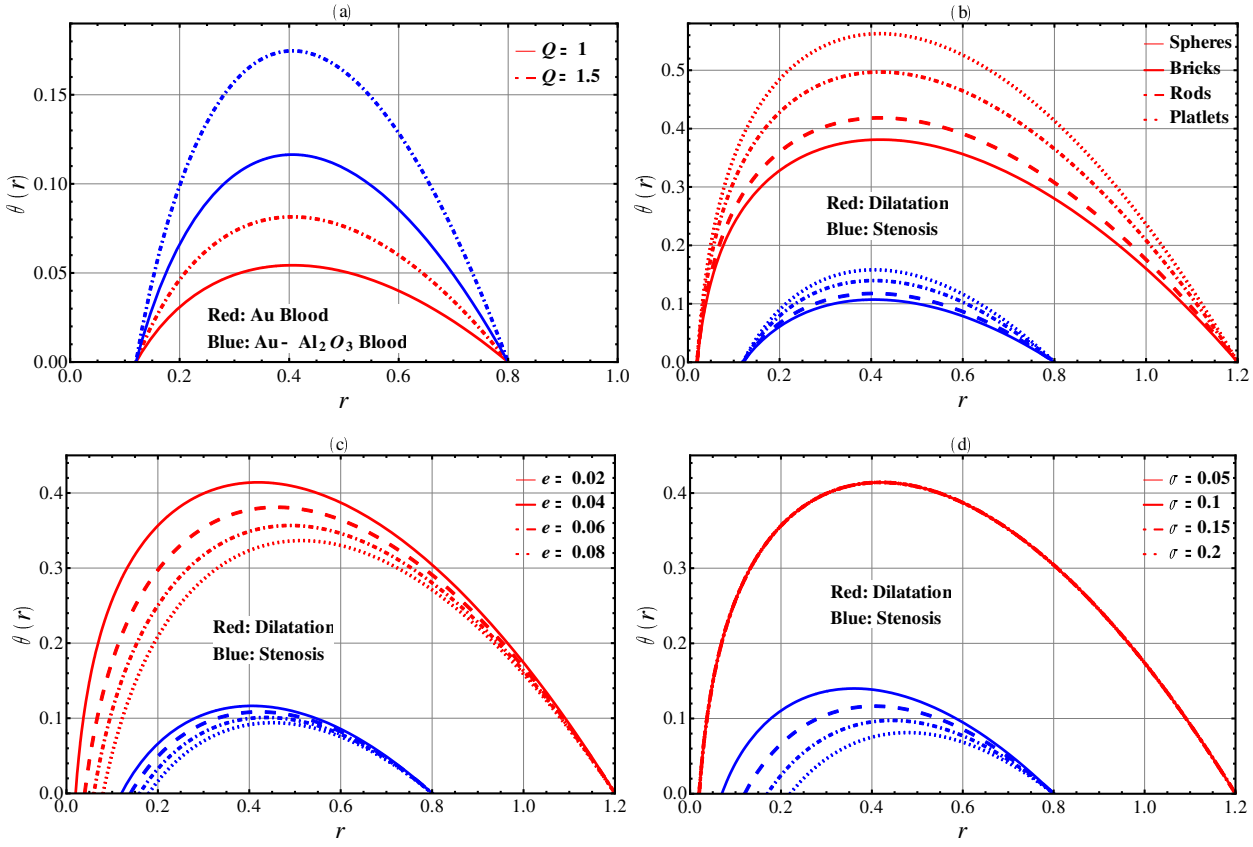

Fig. 2 Temperature $\theta(r)$ against the radial coordinate r

6.2 Hemodynamic Velocity

Fig. 3 is showing hemodynamic velocity against r for different values of relaxation time parameter λ_1, fractional parameter α, Grashof number parameter G_r, catheter's radius parameter e, catheter's maximum height parameter σ and nanoparticles shape factor n. In Fig. 3 a comparison is made up between hybrid nanofluid and nanofluid, and between stenosis and aneurysm. In Fig. 3(a) it is discovered that the hemodynamic velocity for nanofluid is much lower than that of hybrid nanofluid. Also by increasing λ_1 hemodynamic velocity decreases. It is observed in Figs. 3(b) and 3(c) that the hemodynamic velocity increases by increasing α and G_r. Also the hemodynamic velocity in stenosis segment is much lower than that of dilatation segment. Figs. 3(d) and 3(f) show that the velocity decreases by decreasing nanoparticles shape factor n and by increasing e. Moreover it is observed that hemodynamic velocity in stenosis segment is much lower than that of dilatation segment. Fig. 3(e) shows that the hemodynamic velocity decreases by increasing σ in stenosis segment while remains unchanged in dilatation segment. And hemodynamic velocity is higher in dilatation segment as compared to stenosis segment.

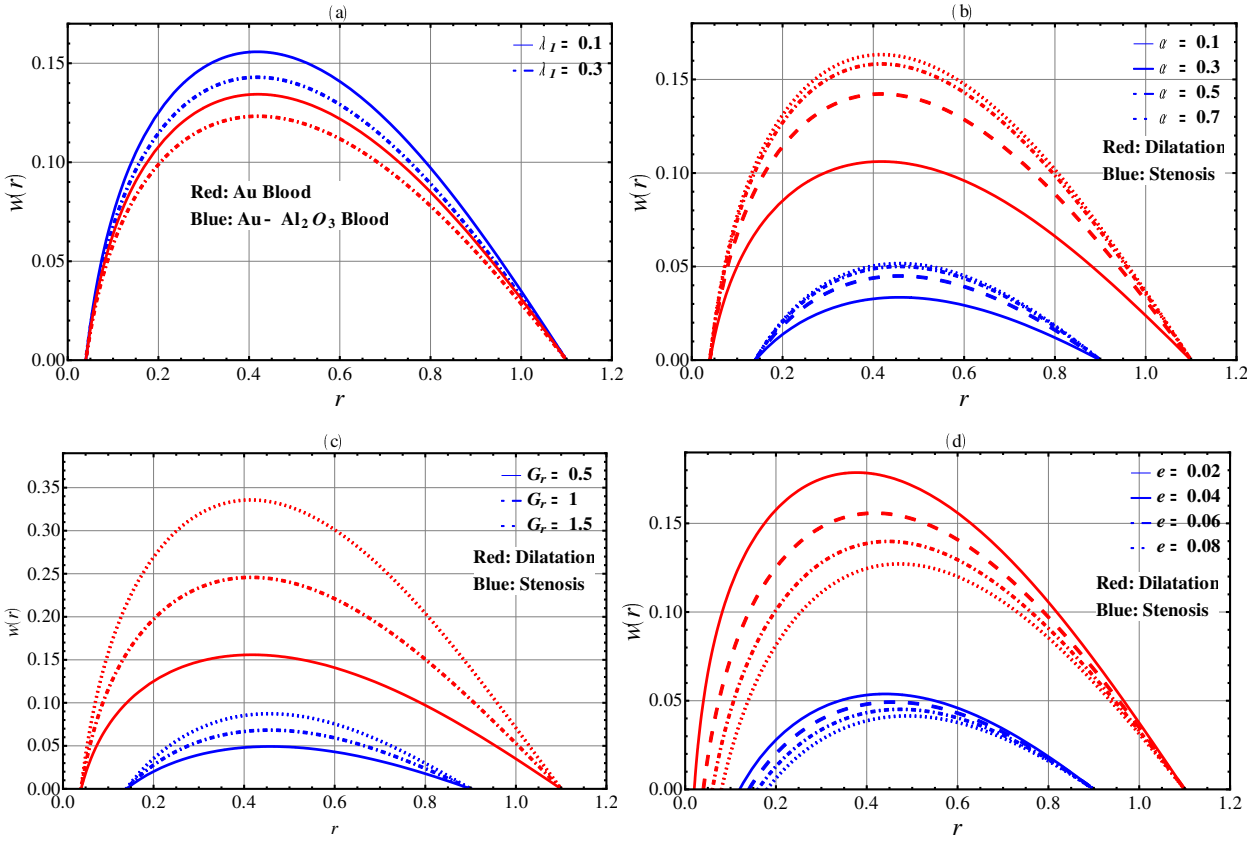

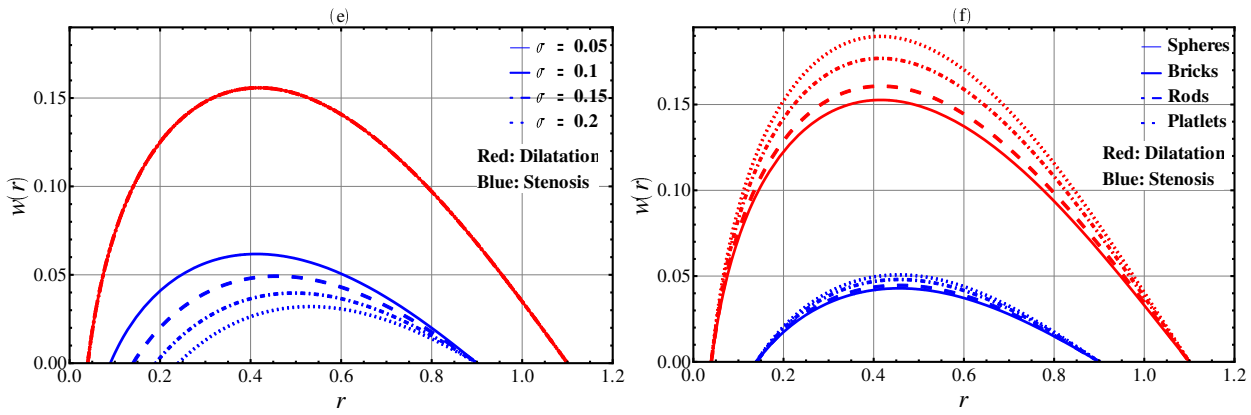

Fig. 3 Hemodynamic velocity $w(r)$ against the radial coordinate r

6.3 Wall Shear Stress (WSS)

The WSS is important to comprehend the movement of the infection in the artery because of the connection between the restriction of arteriosclerosis (dilatation/ stenosis) and the catheter wall or arterial wall. Figs. 4(a) to 4(d) are setup to show the changes in WSS on arterial wall segment (τ_R) for different parameters for stenotic and aneurysmal segments. Figs. 5 (a) to 5(d) are setup to show the changes in WSS on catheter wall segment (τ_χ) for different parameters of interest for stenotic and aneurysmal segments. A contrary conduct is seen for stenotic and aneurysmal segment.

6.3.1 Wall Shear Stress (τ_R) on Arterial Wall Segment

In Fig. 4 for stenotic segment, it is significant to note that τ_R (β_1 to $\beta_1 + L_0$) begins expanding towards the upstream of the stenotic section (i.e. $z = \beta_1$) to move toward its maximal value (i.e. $z = \beta_1 + \frac{L_0}{2}$) and afterward begins steeply diminishing from its maximal value towards the downstream and attains it minimal value (i.e. $z = \beta_1 + L_0$) of the stenotic segment. Presently, for the aneurysmal segment τ_R (β_2 to $\beta_2 + L_0$) begins steeply diminishing towards the downstream of the aneurysmal section (i.e. $z = \beta_2$) to move toward its base worth (i.e. $z = \beta_2 + \frac{L_0}{2}$) and afterward begins quickly expanding from its base an incentive towards the finish of the aneurysmal segment (i.e. $z = \beta_2 + L_0$).

In Figs. 4 arterial wall shear stress τ_R is plotted against z for different values of fractional parameter α, relaxation time parameter λ_1, catheter's radius parameter e and catheter's maximum height parameter σ. Fig. 4(a) shows that τ_R decreases by increasing α in stenosis segment. And τ_R increases by increasing α in dilatation segment. Figs. 4(b) and 4(c) show that τ_R increases by increasing λ_1 and e in stenosis segment. And τ_R decreases by increasing λ_1 and e in dilatation

segment. It is seen in Fig. 4(d) that τ_R increases by increasing σ in stenosis segment. And τ_R remains unchanged by increasing σ in dilatation segment. An opposite behavior of τ_R is observed in stenosis and dilatation segments.

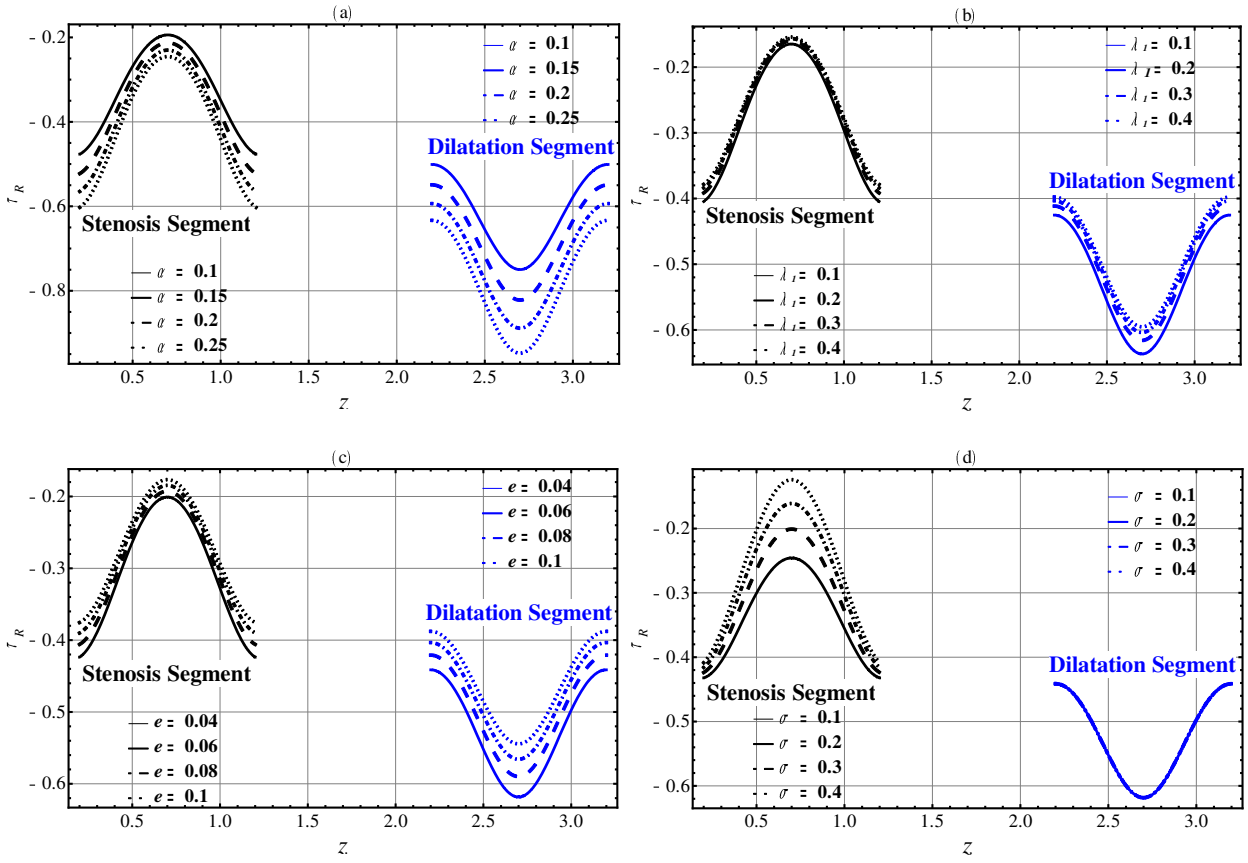

Fig. 4 Wall shear stress τ_R against axial distance z

6.3.2 Wall Shear Stress (τ_χ) on Catheter Wall Segment

In Fig. 5 for stenotic segment, it is significant to note that τ_χ (β_1 to $\beta_1 + L_0$) begins steeply diminishing towards the downstream of the stenotic section (i.e. $z = \beta_1$) to move toward its base worth (i.e. $z = \beta_1 + \frac{L_0}{2}$) and afterward begins quickly expanding from its base an incentive towards the finish of the stenotic segment (i.e. $z = \beta_1 + L_0$). Presently, for the aneurysmal segment τ_χ (β_2 to $\beta_2 + L_0$) begins expanding towards the upstream of the aneurysmal section (i.e. $z = \beta_2$) to move toward its maximal value (i.e. $z = \beta_2 + \frac{L_0}{2}$) and afterward begins steeply diminishing from its maximal value towards the downstream and attains it minimal value (i.e. $z = \beta_2 + L_0$) of the aneurysmal segment.

In Fig. 5 catheter wall shear stress τ_χ is plotted against z for different values of fractional parameter α, relaxation time parameter λ_1, catheter's radius parameter e and catheter's maximum height parameter σ. Fig. 5(a) shows that τ_χ increases by increasing α in stenosis segment. And τ_χ decreases by increasing α in dilatation segment. Figs. 5(b) and 5(c) show that τ_χ decreases by increasing λ_1 and e in stenosis segment. And τ_χ increases by increasing λ_1 and e in dilatation segment. It is seen in Fig. 5(d) that τ_χ increases by increasing σ in stenosis segment. And τ_χ remains unchanged by increasing σ in dilatation segment. An opposite behavior of τ_χ is observed in stenosis and dilatation segments.

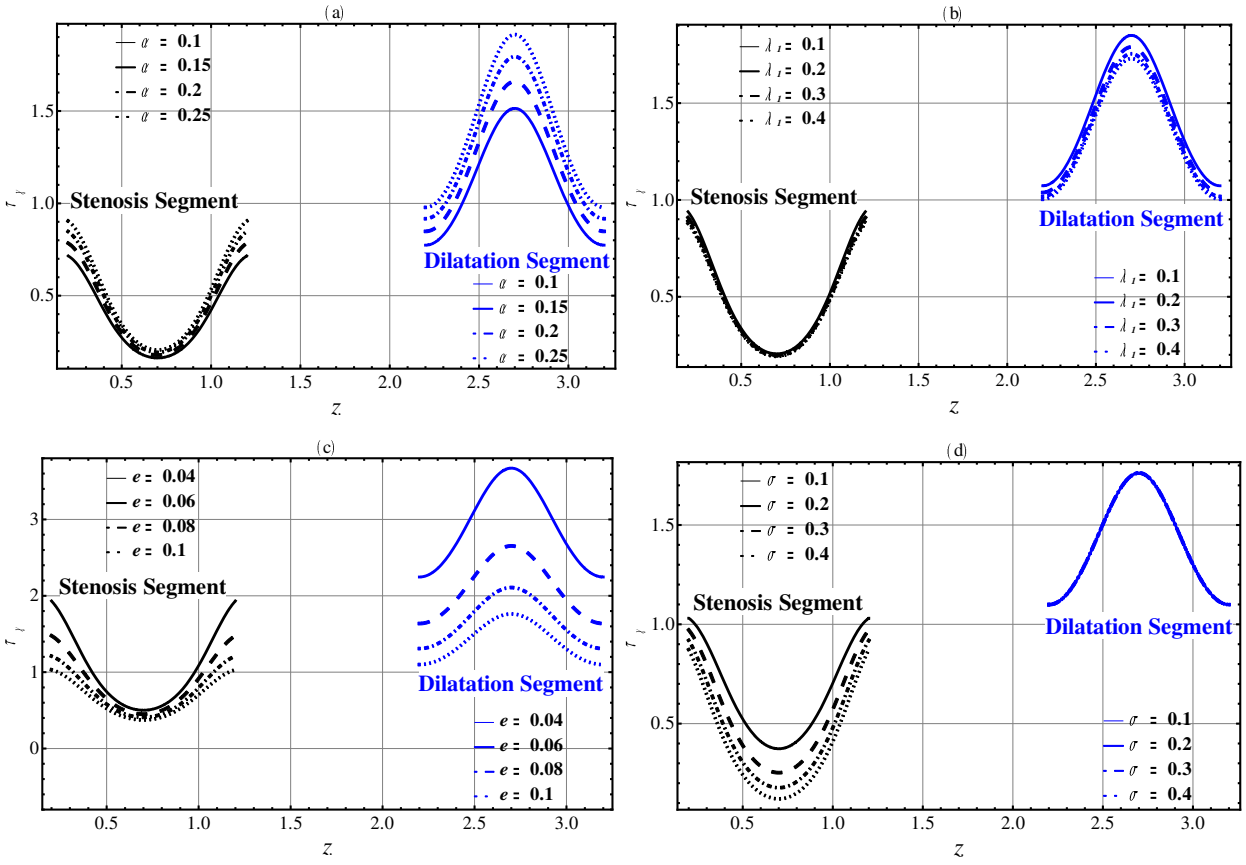

Fig. 5 Wall shear stress τ_χ against axial distance z

6.4 Resistance Impedance

In Fig. 6 the resistance impedance λ against the maximum height a for stenosis and aneurysm in the presence of catheter is plotted. Resistance impedance λ for different values of fractional parameter α, relaxation time parameter λ_1, hybrid nanoparticles fractional parameters ϕ_1 and ϕ_2, catheter's radius parameter e and catheter's maximum height parameter σ is plotted. For both stenosis and aneurysm segments, it is discovered that resistance impedance λ is inversely

proportional to a. It's also worth noting that for maximal a, the resistance impedance λ for stenosis is higher than for aneurysm. In Figs. 6(a) and 6(b) it is observed that by increasing fractional parameter α resistance impedance λ decreases. And resistance impedance for stenosis segment is higher than that of dilatation segment. Figs. 6(c)-6(h) show that the resistance impedance λ increases by increasing relaxation time parameter λ_1, hybrid nanoparticles fractional parameters ϕ_1 and ϕ_2 and catheter's radius parameter e. Moreover, resistance impedance for stenosis segment is higher as compared to dilatation segment. It is seen in Figs. 6(i) and 6(j) that by increasing catheter's maximum height parameter σ resistance impedance λ increases in stenosis segment and remains unchanged in dilatation segment. It is also observed that resistance impedance for stenosis segment is higher as compared to dilatation segment.

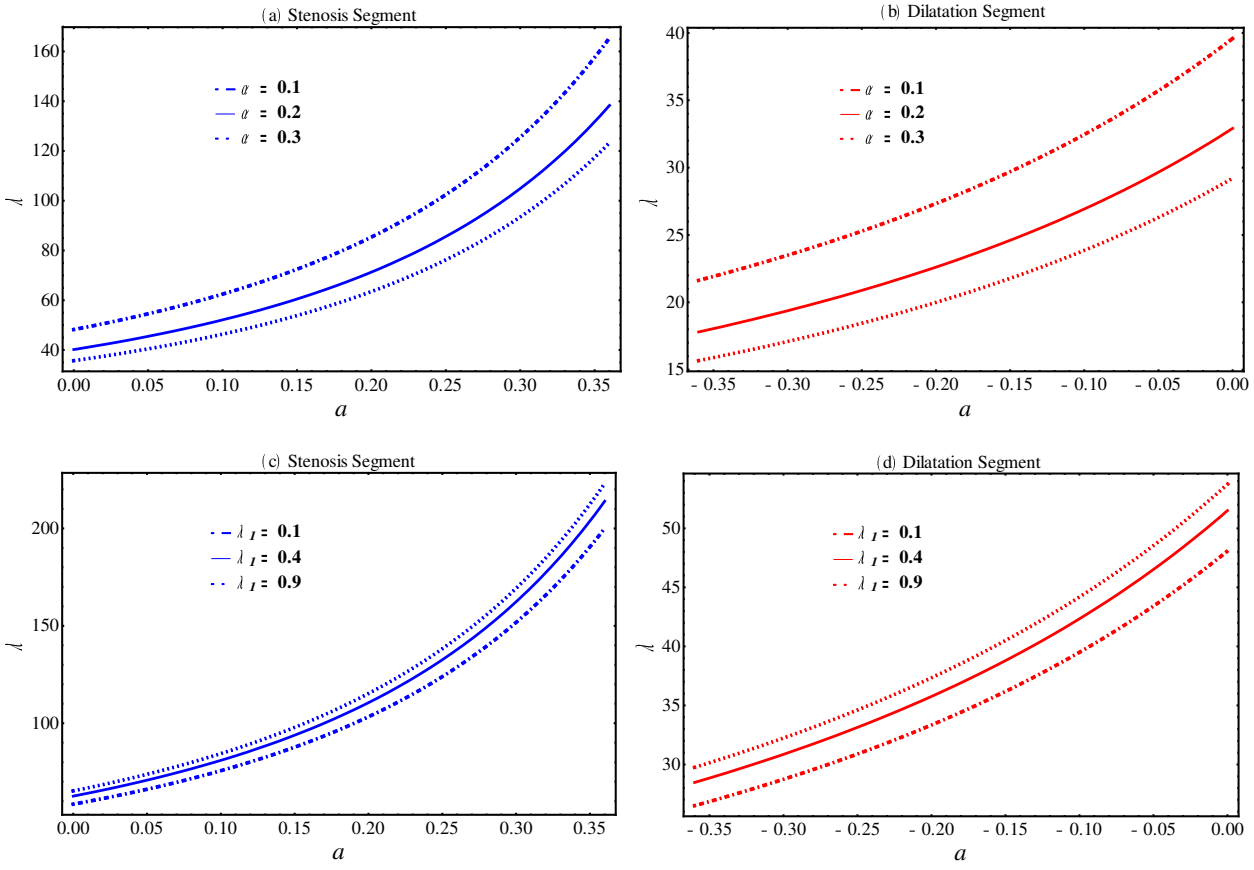

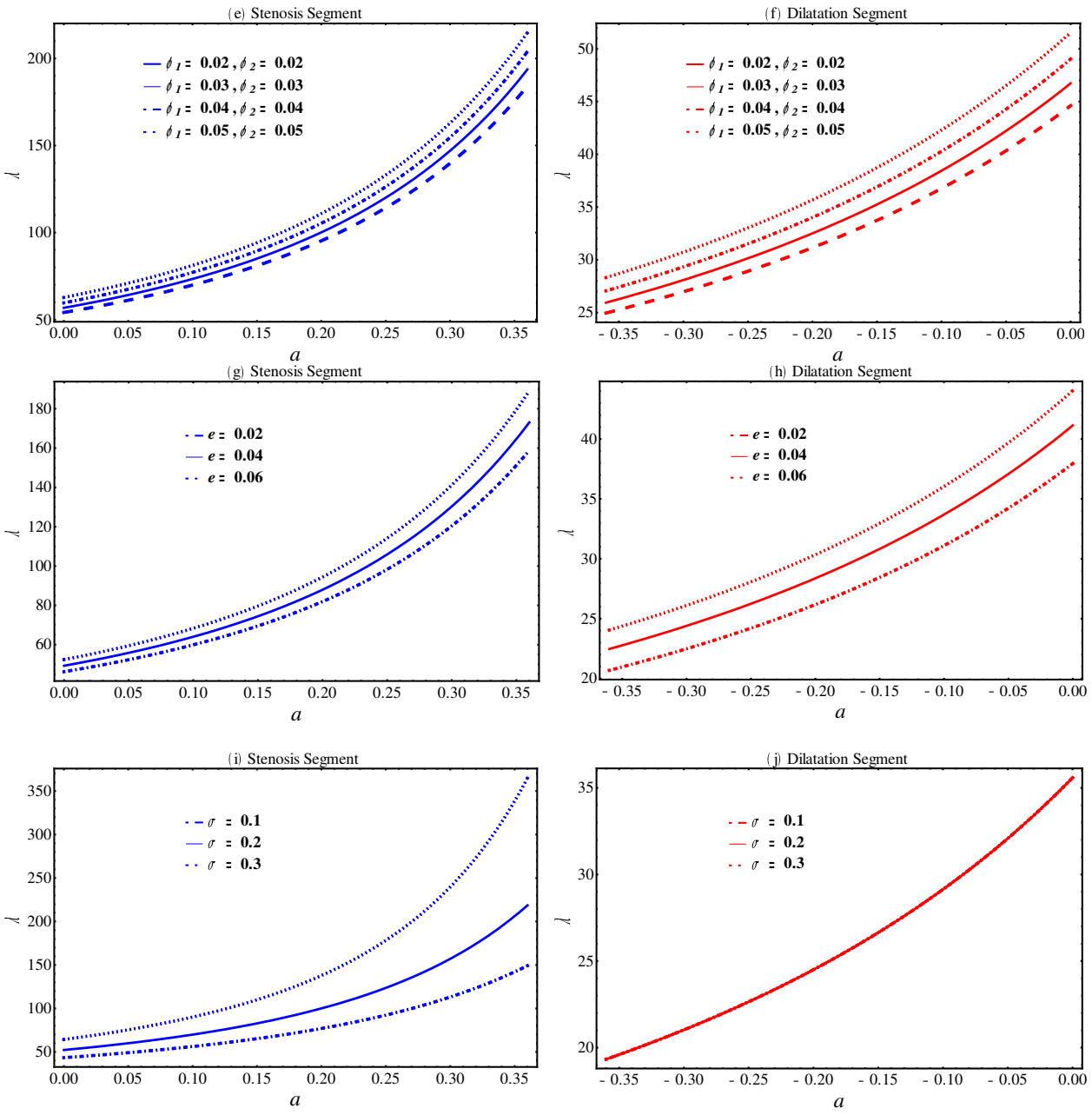

Fig. 6 Resistance impedance λ against a

6.4 Trapping

The trapping is a significant in connection to the hydrodynamic characteristics of aneurysm and stenosis segments. Drawing contours is the best way to imagine the trapping process. The trapping mechanism is distributed through the revolving bolus internally. The streamlines are enclosed by the scale of the flowing bolus in the fluid. The trapping mechanism for maximum height of stenosis and aneurysm a, catheter's radius e and catheter's maximum height σ are discussed for both stenosis and aneurysm segment. It is observed in Fig.7 that the rotated bolus

sized increased by increasing a, e and σ in stenosis segment. It is found in Fig. 8 that the circulating bolus size increases by increasing a in dilatation segment. Moreover it is also seen that size of the circulating bolus decreases by increasing e in dilatation segment. It is also observed that size of circulation bolus remains unchanged by increasing σ in dilatation segment.

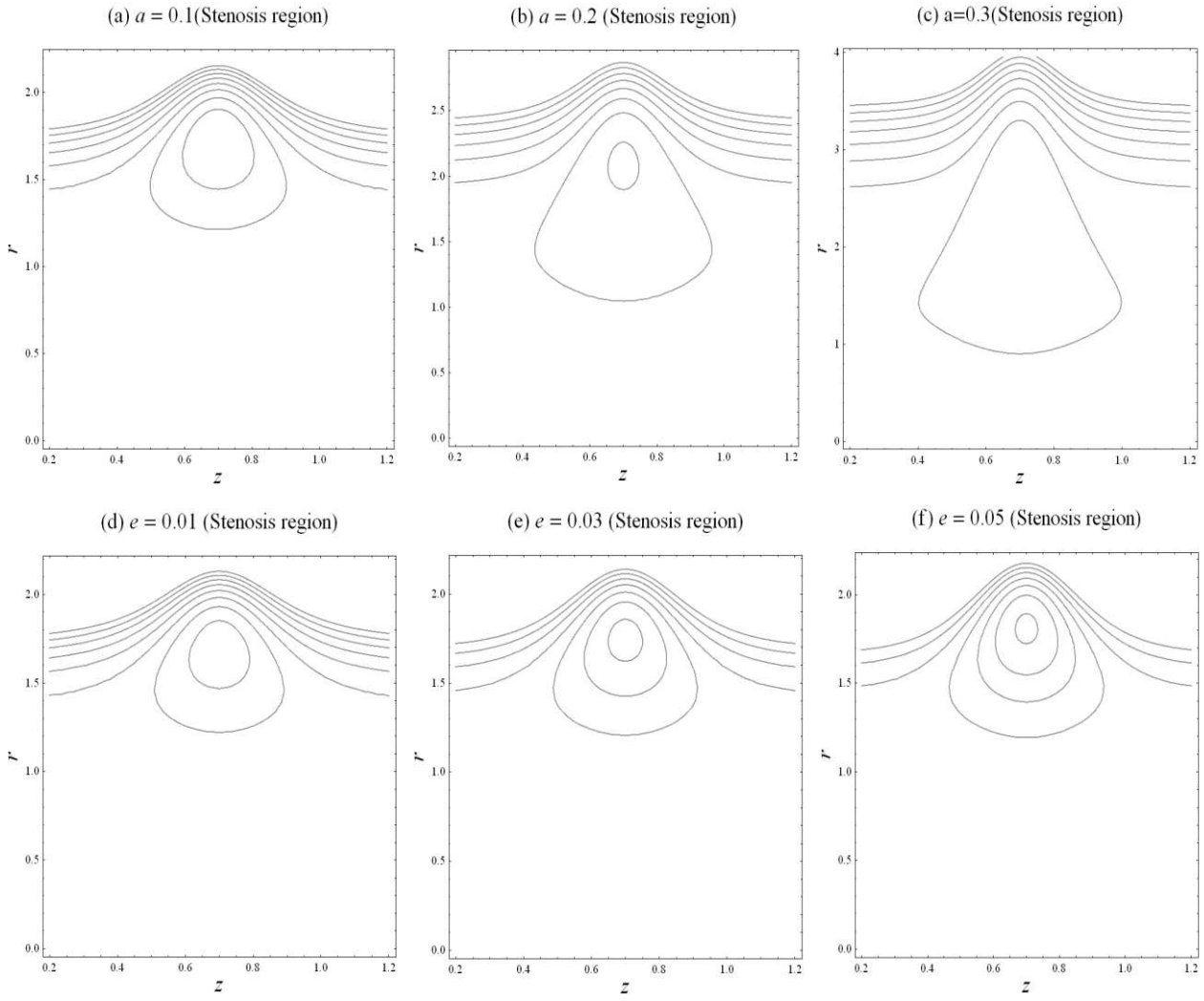

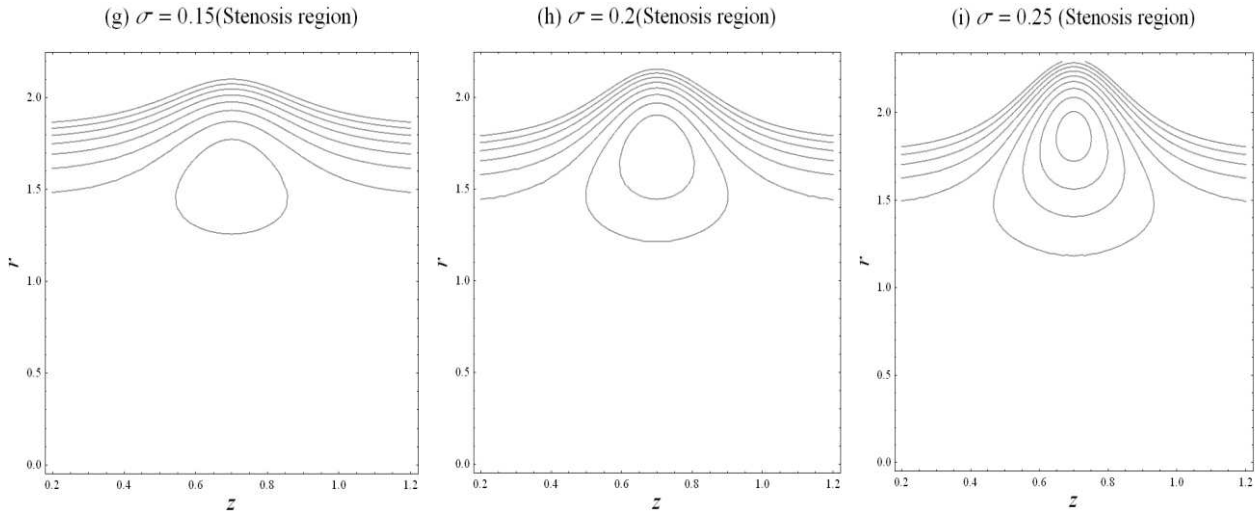

Fig. 7 Streamlines with z in stenosis segment

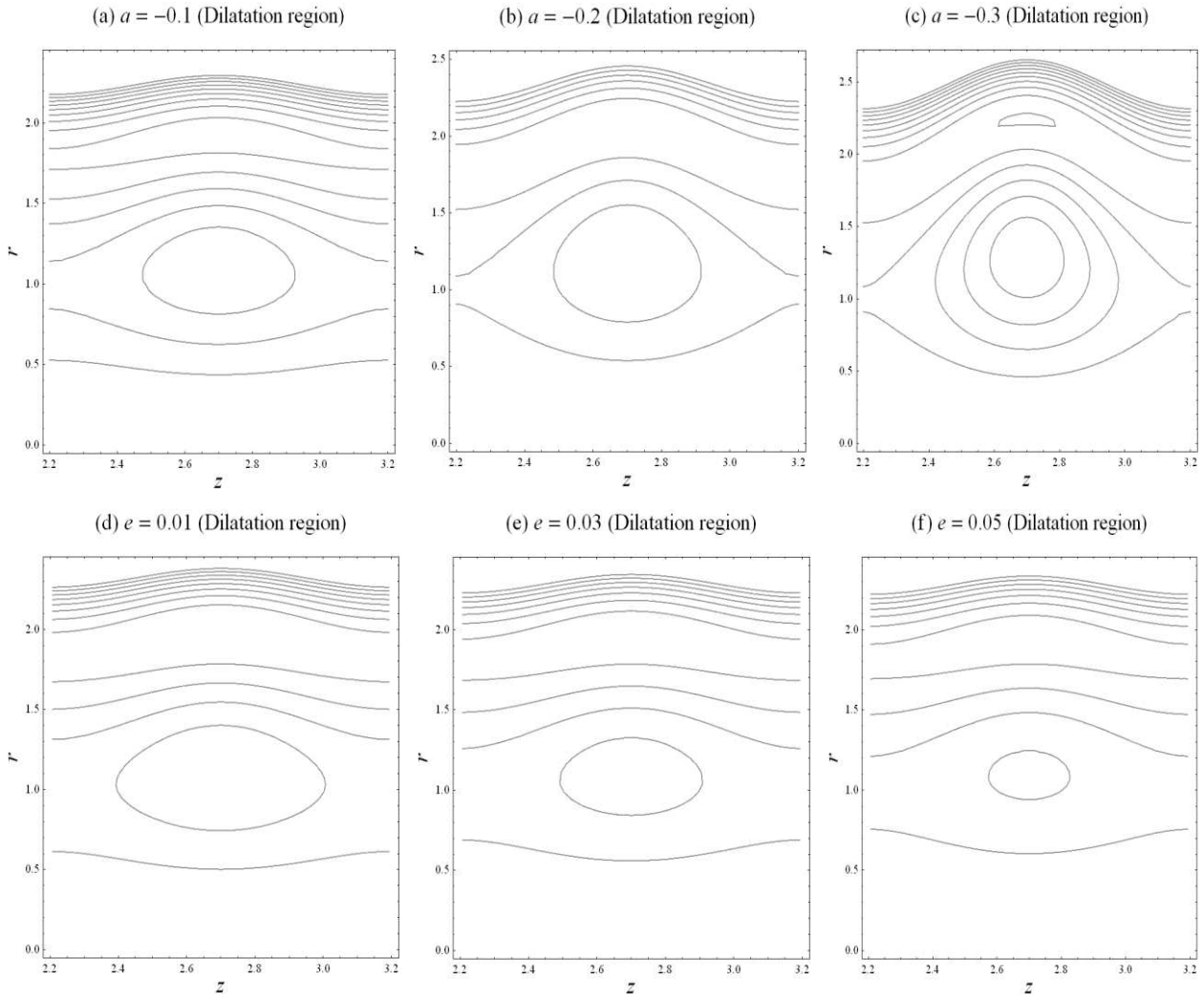

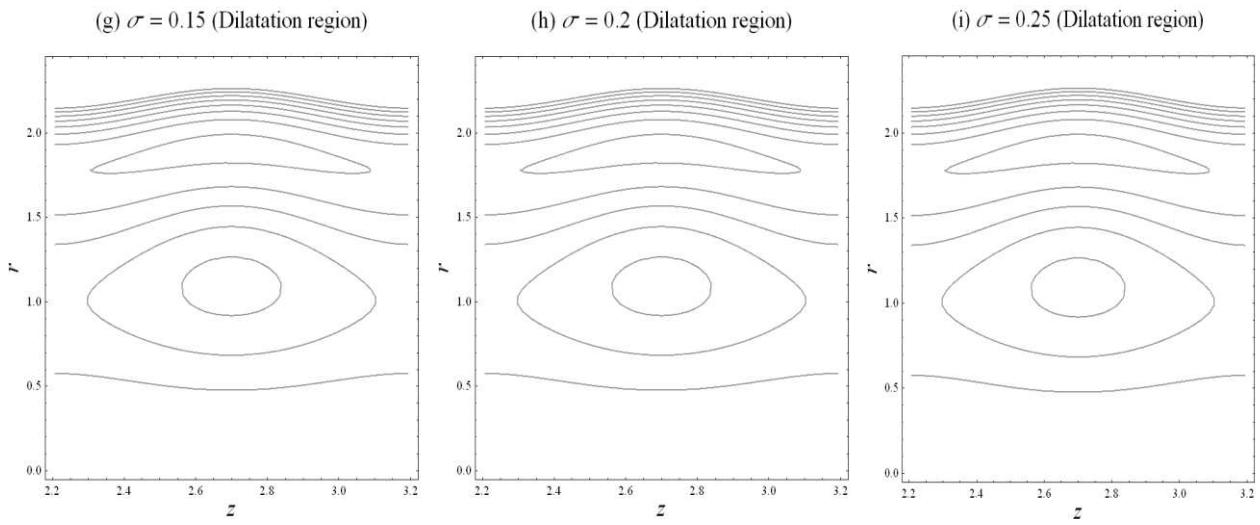

Fig. 8 Streamlines with z in dilatation segment

7. Conclusion

In this paper hybrid fractional second-grade nano blood flow through concentrically catheterized stenosed and aneurysmal arterial segment is studied. Exact solutions are obtained by solving governing equations, and the effects of the relevant parameters are examined. Comparisons are established for aneurysm and stenosis, and for hybrid nanofluid and nanofluid. The principle discoveries from the graphical portrayals can be summed up as follows:

- As spherical-shaped nanoparticles are compared to other shapes of nanoparticles, the temperature drops.
- Temperature for dilatation segment is higher than that of stenosis segment.
- Hybrid nanofluid heat transfer is higher than nanofluid heat transfer.
- As compared to nanofluid, the hemodynamic velocity of hybrid nanofluid is higher.
- As compared to the other nanoparticles' forms, the velocity diminishes for spherical-shaped nanoparticles.
- Hemodynamic velocity for dilatation segment is higher than that of stenosis segment.
- The arterial wall shear stress in the stenosis segment increases quickly to its greatest value and then begins to decrease steeply to the end of the stenosis segment, whereas the opposite trend of arterial wall shear stress is detected in the aneurysmal segment when compared to the stenosis segment.
- The catheter wall shear stress in the aneurysmal segment increases quickly to its greatest value and then begins to decrease steeply to the end of the aneurysmal segment, whereas the opposite trend of catheter wall shear stress is detected in the stenotic segment when compared to the aneurysmal segment.
- Contrary behavior of wall shear stress is observed on arterial and catheter wall segment.

- Wall shear stress on catheter wall segment is more than that of wall shear stress on arterial wall segment.
- For the stenosis, the resistance impedance achieves a higher value than for the aneurysm segment.
- The trapping mechanism depicts the formation of a rotating bolus in the stenotic and aneurysmal segments with varying parameters of concentration.

References:

[1] O.U. Mehmood, N. Mustapha, S. Shafie, Unsteady two dimensional blood flow in porous artery with multi-irregular stenosis. Transport in Porous Media 92 (2012) 259-275.

[2] B. Pincombe, J. Mazumdar, The effects of Post-Stenotic Dilatations on the flow of a Blood Analogue through Stenosed Coronary Arteries, Math. Comput. Modelling 25 (1997) 57–70.

[3] S. Nadeem, S. Ijaz, Influence of metallic nanoparticles on blood flow through arteries having both stenosis and aneurysm, IEEE Trans. Nanobiosci. 14 (2015) 668–679, https://doi.org/10.1109/TNB.2015.2452932.

[4] R. Ellahi, S. Rahman, S. Nadeem, Blood flow of Jeffrey fluid in a catharized tapered artery with the suspension of nanoparticles, Phys. Lett. A 378 (2014)2973–2980.

[5] Kh.S. Mekheimer, A.Z. Zaher, A.I. Abdellateef, Entropy hemodynamics particle-fluid suspension model through eccentric catheterization for time-variant stenoticarterial wall: Catheter injection, Int. J. Geom. Meth. Mod. Phys. 16 (11) (2019) 1950164, https://doi.org/10.1142/S0219887819501640 29.

[6] A.R. Mantha, G. Benndorf, A. Hernandez, R.W. Metcalfe, Stability of pulsatile blood flow at the ostium of cerebral aneurysms, J. Biomech. 42 (2009) 1081–1087

[7] S.I. Abdelsalam, K. Vafai, Particulate suspension effect on peristaltically induced unsteady pulsatile flow in a narrow artery: blood flow model, Math. Biosci. 283 (2017) 91–105.

[8] I. Shahzadi, N. Ahsan, S. Nadeem, Analysis of bifurcation dynamics of streamlines topologies for pseudoplastic shear thinning fluid: Biomechanics application, Physica A (2019), https://doi.org/10.1016/j.physa.2019.122502.

[9] Sara I. Abdelsalama, Kh.S. Mekheimer, A.Z. Zaher, Alterations in blood stream by electroosmotic forces of hybrid nanofluid through diseased artery: Aneurysmal/stenosed segment, Chinese Journal of Physics 67 (2020) 314–329.

[10] R.K. Dash, G. Jayaraman, K.N. Mehta, Flow in a catheterized curved artery with stenosis, J. Biomech. 49 (1999) 61.

[11] V.P. Srivastava, R. Rastogi, Blood flow through a stenosed catheterized artery: effects of hematocrit and stenosis shape, Comput. Math. Appl. 59 (4) (2010) 1377–1385.

[12] K.S. Mekheimer, M.A. El Kot, Mathematical modeling of axial flow between two eccentric cylinders: application on the injection of eccentric catheter through stenotic arteries, Int. J. Non-Lin. Mech. 47 (8) (2012) 927–937.

[13] J.V. Ramana Reddy, D. Srikanth, S.V.S.S.N.V.G. Krishna Murthy, Mathemat- ical modelling of pulsatile flow of blood through catheterized unsym- metric stenosed artery—effects of tapering angle and slip velocity, Eur. J. Mech–B/Fluids 48 (2014) 236–244.

[14] K.S. Mekheimer, M.A.E. Kot, Suspension model for blood flow through catheter-ized curved artery with time-variant overlapping stenosis, Eng. Sci. Technol. Int. J. 18 (3) (2015) 452–462.

[15] D. Srikanth, J.V. Ramana Reddy, S. Jain, A. Kale, Unsteady polar fluid model of blood flow through tapered -shape stenosed artery: effects of catheter and velocity slip, Ain Shams Eng. J. 6 (3) (2015) 1093–1104.
[16] Akbar Zaman, Nasir Ali, O. Anwar Beg, Numerical simulation of unsteady micropolar hemodynamics in a tapered catheterized artery with a combination of stenosis and aneurysm, Med Biol Eng Comput (2016) 54:1423–1436.
[17] O.U. Mehmood**,** M.M. Maskeen, A. Zeeshan, M. Hassan, Heat transfer enhancement in hydromagnetic alumina-copper/water hybrid nanofluid flow over a stretching cylinder, Journal of Thermal Analysis and Calorimetry, 138, 1127–1136, 2019. https://doi.org/10.1007/s10973-019-08304-7.
[18] O.U. Mehmood, M. Marin, M.M. Maskeen, A. Zeeshan and M. Hassan, Hydromagnetic transport of iron nanoparticle aggregates suspended in water, Indian J Phys (January 2019) 93(1):53–59.
[19] O.U. Mehmood, Hydromagnetic nanofluid flow past a stretching cylinder embedded in non-Darcian Forchheimer porous media. Neural Computing & Applications, (Neural Comput & Applic) (2018) 30:3479–3489.
[20] S.I. Abdelsalam, M.M. Bhatti, New insight into AuNP applications in tumor treatment and cosmetics through wavy annuli at the nanoscale, Sci. Rep. 9 (2019) 1–14.
[21] S. Das, R.N. Jan, O.D. Makinde, MHD Flow of Cu −; Al2O3 /water hybrid nanofluid in porous channel: analysis of entropy generation, Defect Diffus. Forum 377 (2017) 42–61.
[22] H. Xie, B. Jiang, B. Liu, Q. Wang, J. Xu, F. Pan, An investigation on the tribological performances of the SiO2/MoS2 hybrid nanofluids for magnesium alloy-steel contacts, Nanoscale Res. Lett. 11 (2016) 329–336.
[23] S.P.A. Devi, S.S.U. Devi, Numerical investigation of hydromagnetic hybrid Cu −; Al2O3 /water nanofluid flow over a permeable stretching sheet with suction, Int. J. Nonlinear Sci. Num. Simul. 17 (2016) 249–257.
[24] Kh.S. Mekheimer, W.M. Hasona, R.E. Abo-Elkhair, A.Z. Zaher, Peristaltic blood flow with gold nanoparticles as a third grade nanofluid in catheter: Application ofcancer therapy, Phys. Lett. A 382 (2018) 85–93.
[25] N.S. Akbar, M. Mustafa, Ferromagnetic effects for nanofluid venture through composite permeable stenosed arteries with different nanosize particles, AIP Advances 5 (2015) 077–102.
[26] S.I. Abdelsalam, M.M. Bhatti, The study of non-Newtonian nanofluid with Hall and ion slip effects on peristaltically induced motion in a non-uniform channel, RSC Advances 8 (2018) 7904–7915.
[27] S.I. Abdelsalam, M.M. Bhatti, The impact of impinging TiO2 nanoparticles in Prandtl nanofluid along with endoscopic and variable magnetic field effects on peristaltic blood flow, Multidiscipline Modeling in Mater. Struct. 14 (2018) 530–548.
[28] I. Shahzadi, S. Suleman, S. Saleem, and S. Nadeem, Utilization of Cu-nanoparticles as medication agent to reduce atherosclerotic lesions of a bifurcated artery having compliant walls, Volume 184 (2020) 105-123.
[29] R. Ellahi, Sadiq M. Sait, N. Shehzad, Z. Ayaz, A hybrid investigation on numerical and analytical solutions of electro-magnetohydrodynamics flow of nanofluid through porous media with entropy generation, Int. J. Numer. Methods Heat Fluid Flow 30 (2020) 834–854.
[30] O.U. Mehmood, S. Uddin, M. Mohamad, M.A.H. Mohmad**,** M. Kamardan and R. Roslan,

Natural Heat Transfer Phenomenon in MHD Fractional Second Grade Fluid, Universal Journal of Mechanical Engineering 7(6C): 32-36, 2019, DOI: 10.13189/ujme.2019.071605.

[31] M. Hameed, Ambreen A. Khan, R. Ellahi, M. Raza, Study of magnetic and heat transfer on the peristaltic transport of a fractional second grade fluid in a vertical tube, Engineering Science and Technology, an International Journal, 18 (2015) 496–502.

[32] S. Nadeem, General periodic flows of fractional Oldroyd-B fluid for an edge, Phys. Lett. A 368 (2007) 181–187.

[33] W.C. Tan, W.X. Pan, M.Y. Xu, A note on unsteady flows of a viscoelastic fluid with the fractional Maxwell model between two parallel plates, Int. J. Non Linear Mech. 38 (5) (2003) 645–650.

[34] W. Tan, Xu Mingyu, Unsteady flows of a generalized second grade fluid with the fractional derivative model between two parallel plates, Acta Mechan. Sinica 20 (5) (2004) 471–476.

[35] M. Hameed, A.A. Khan, R. Ellahi, M. Raza, Study of magnetic and heat transfer on the peristaltic transport of a fractional second grade fluid in a vertical tube, Eng. Sci. Technol., an Int. J. 18 (2015) 496–502.

[36] V.P. Rathod, A. Tuljappa, Slip effect on the peristaltic flow of a fractional second grade fluid through a cylindrical tube, Adv. in Appl. Sci. Res. 6 (3) (2015) 101–111.

Figures

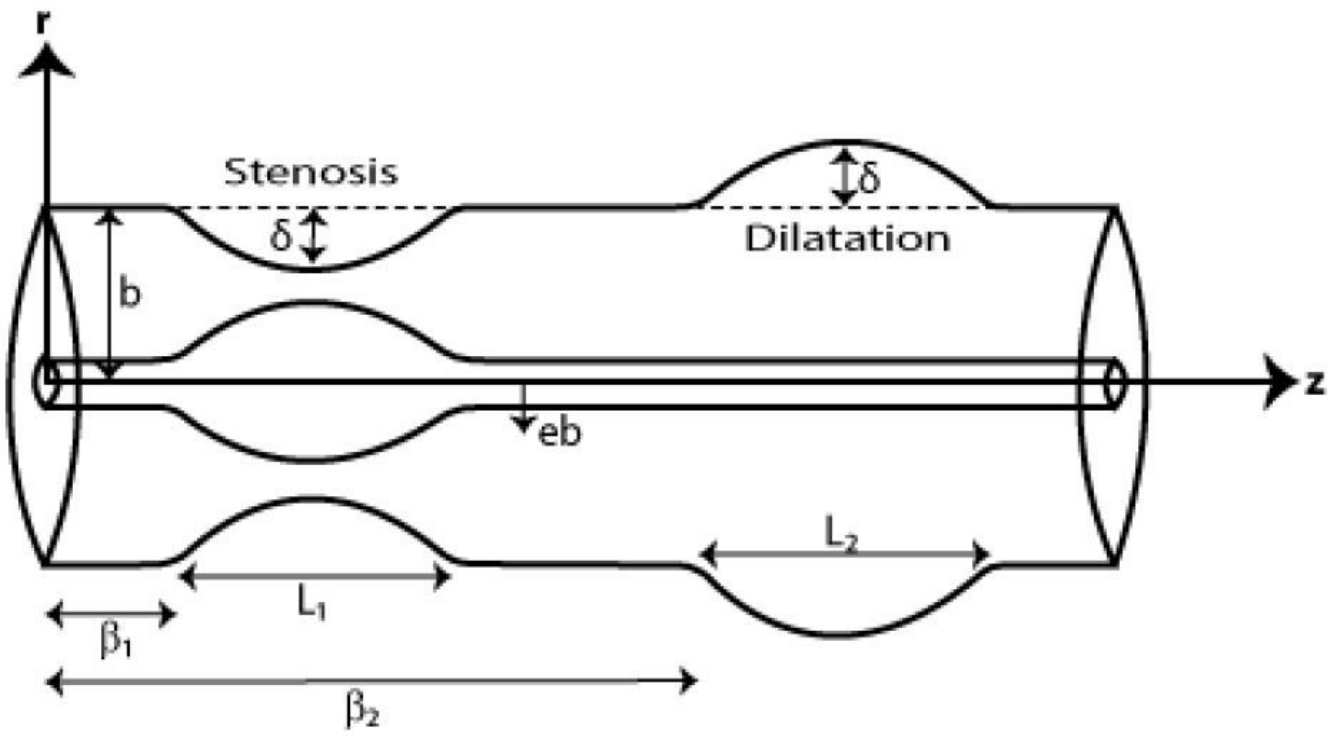

Figure 1

Configuration of the physical model

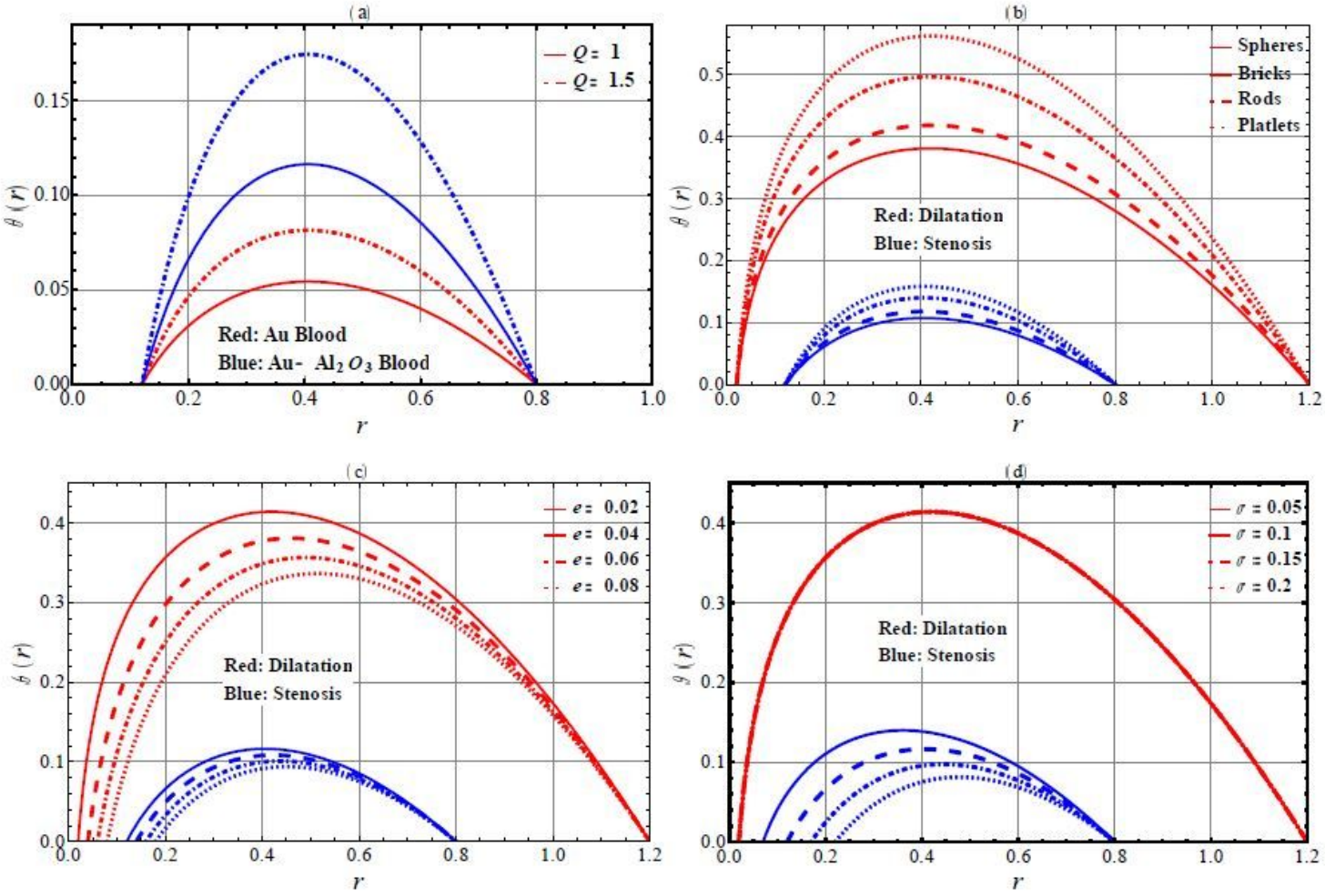

Figure 2

Temperature 0(r) against the radial coordinate r

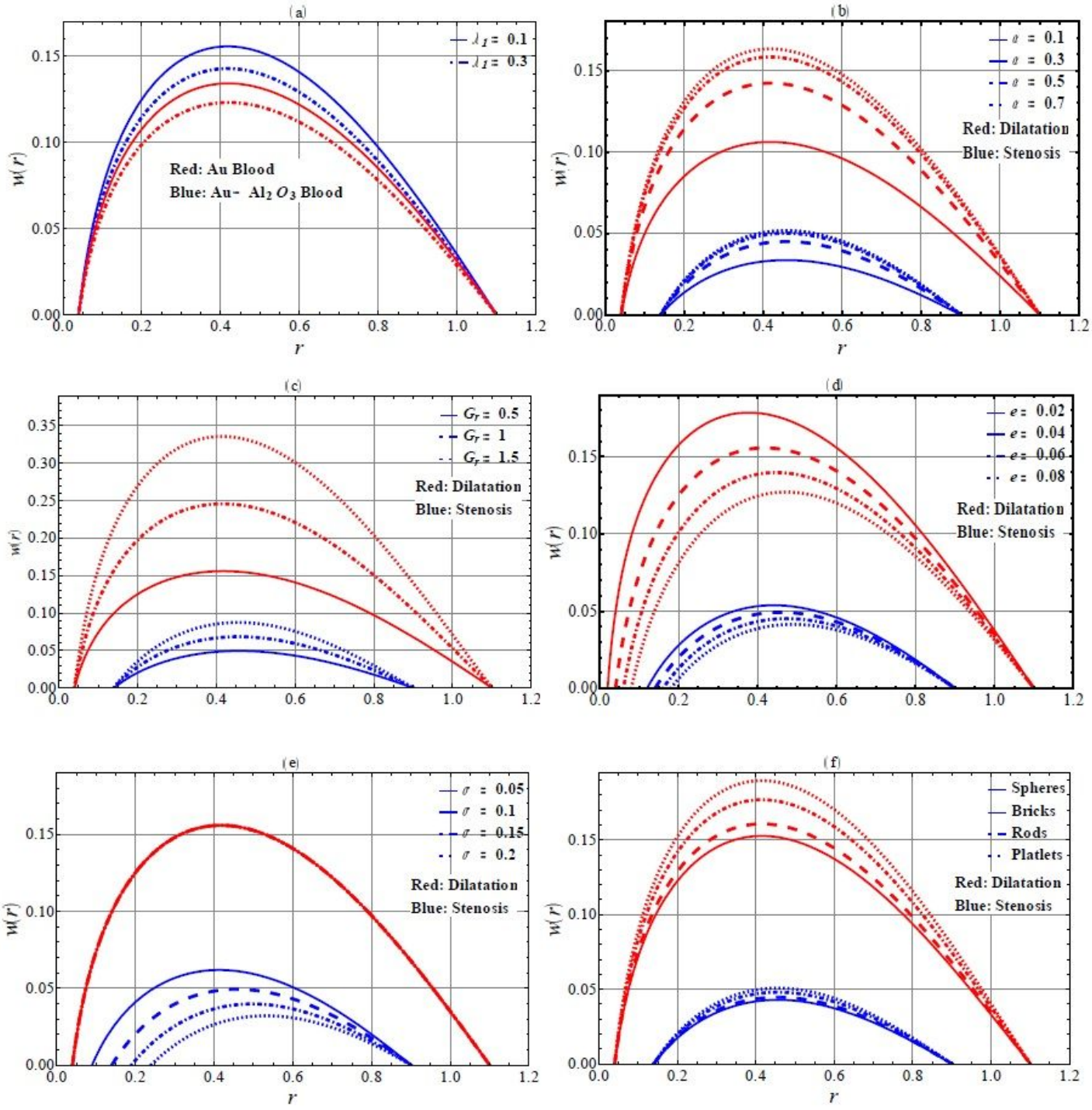

Figure 3

Hemodynamic velocity w(r) against the radial coordinate r

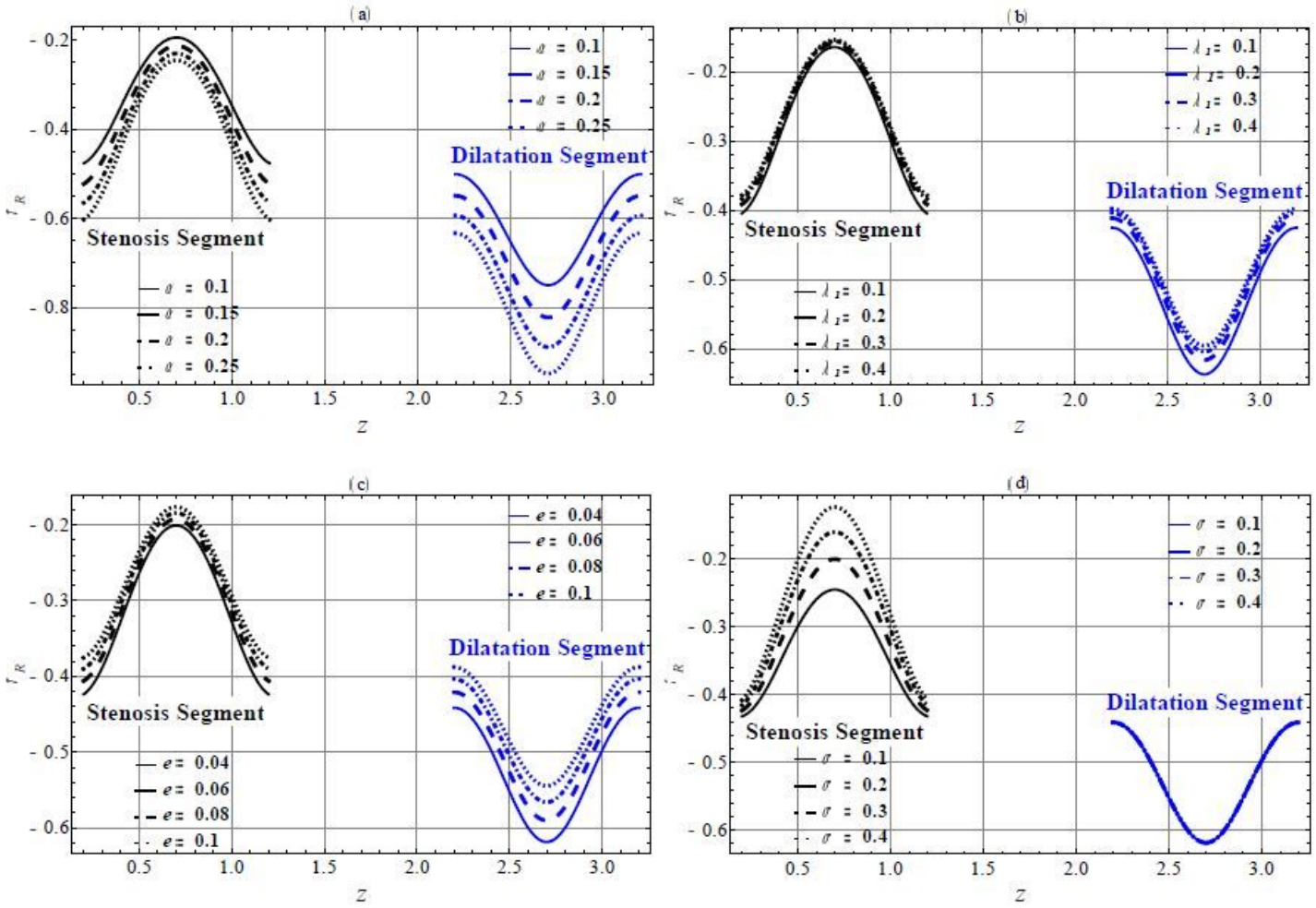

Figure 4

Wall shear stress tr against axial distance z

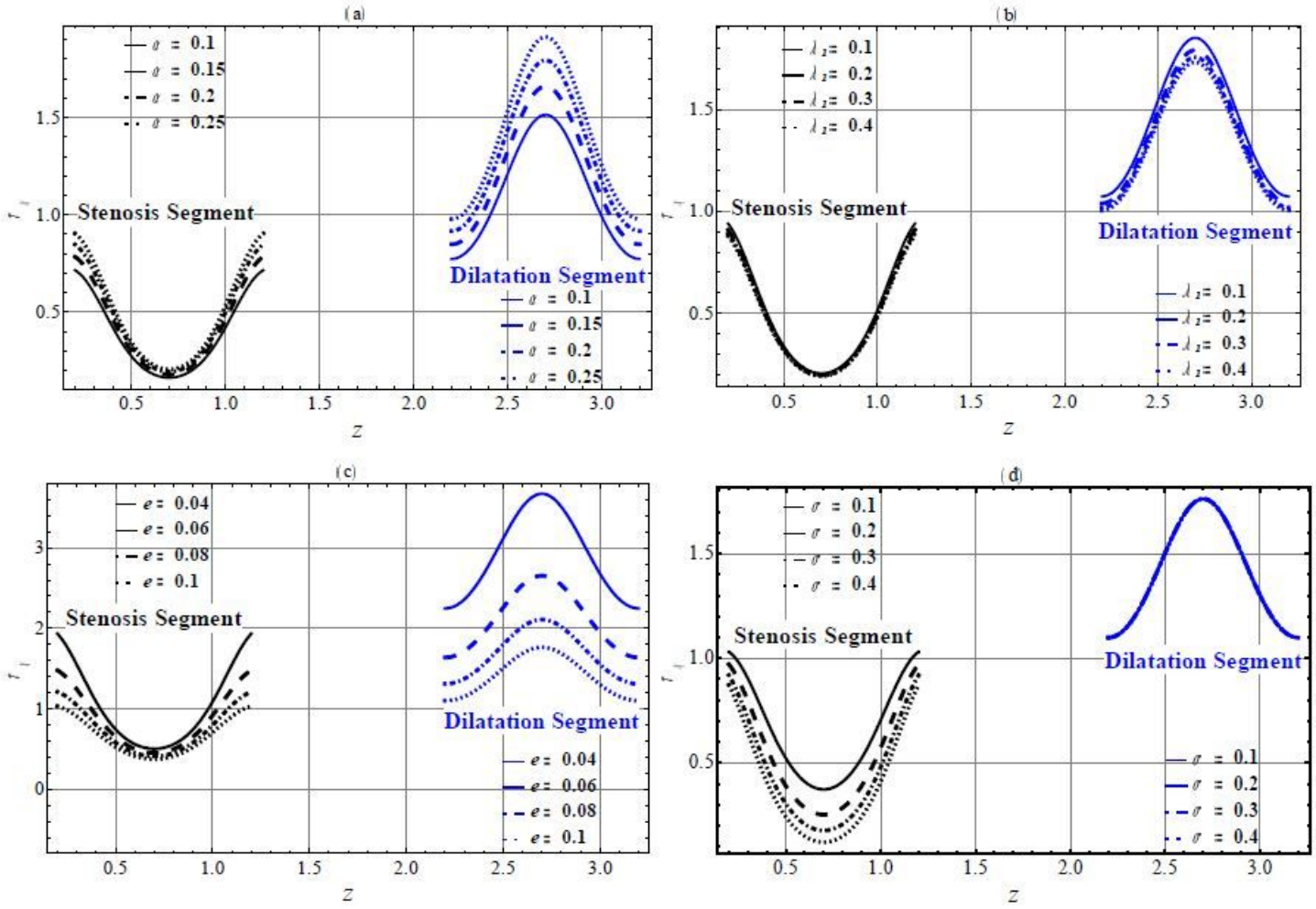

Figure 5

Wall shear stress tx against axial distance z

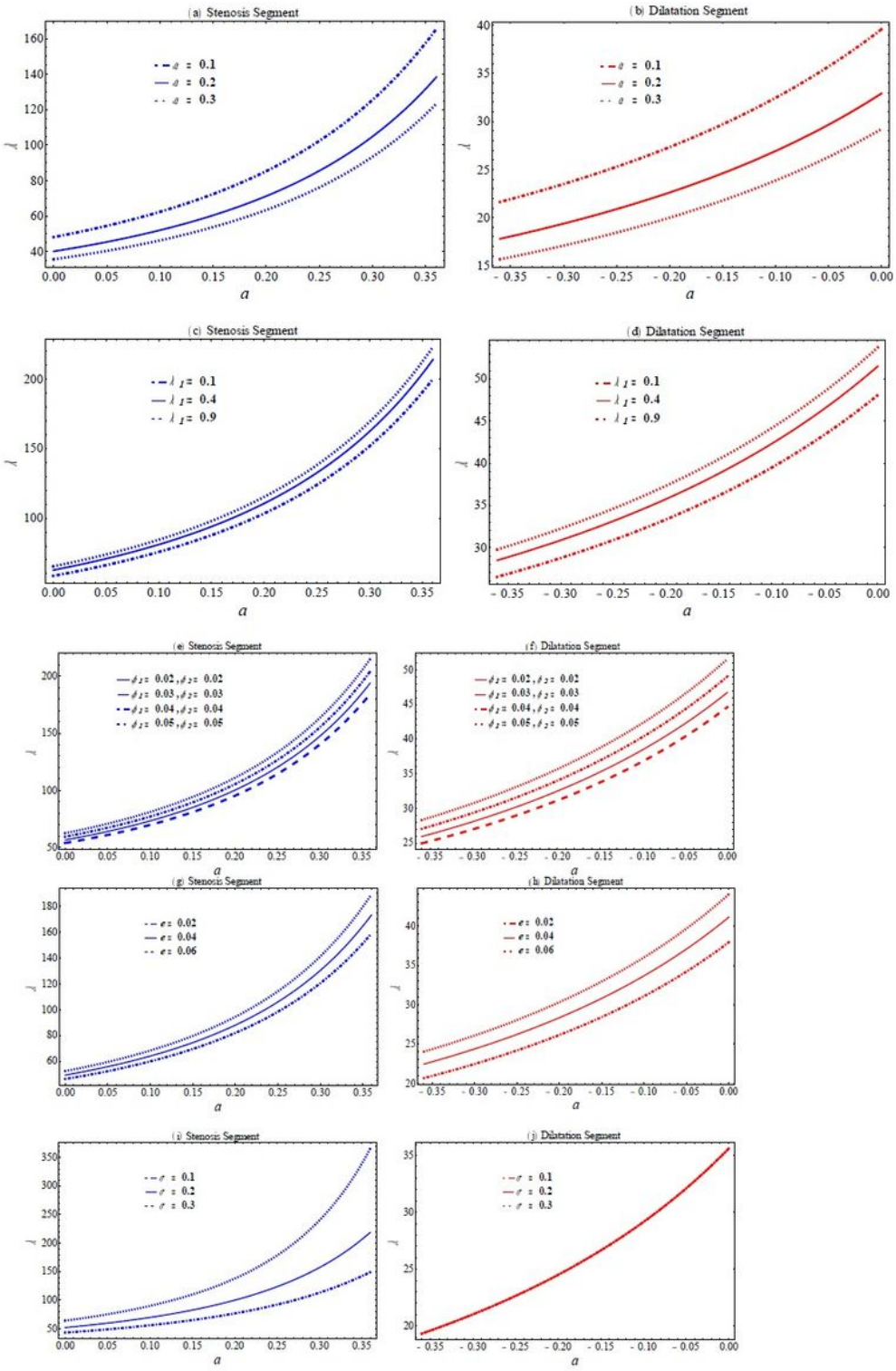

Figure 6

Resistance impedance λ against a

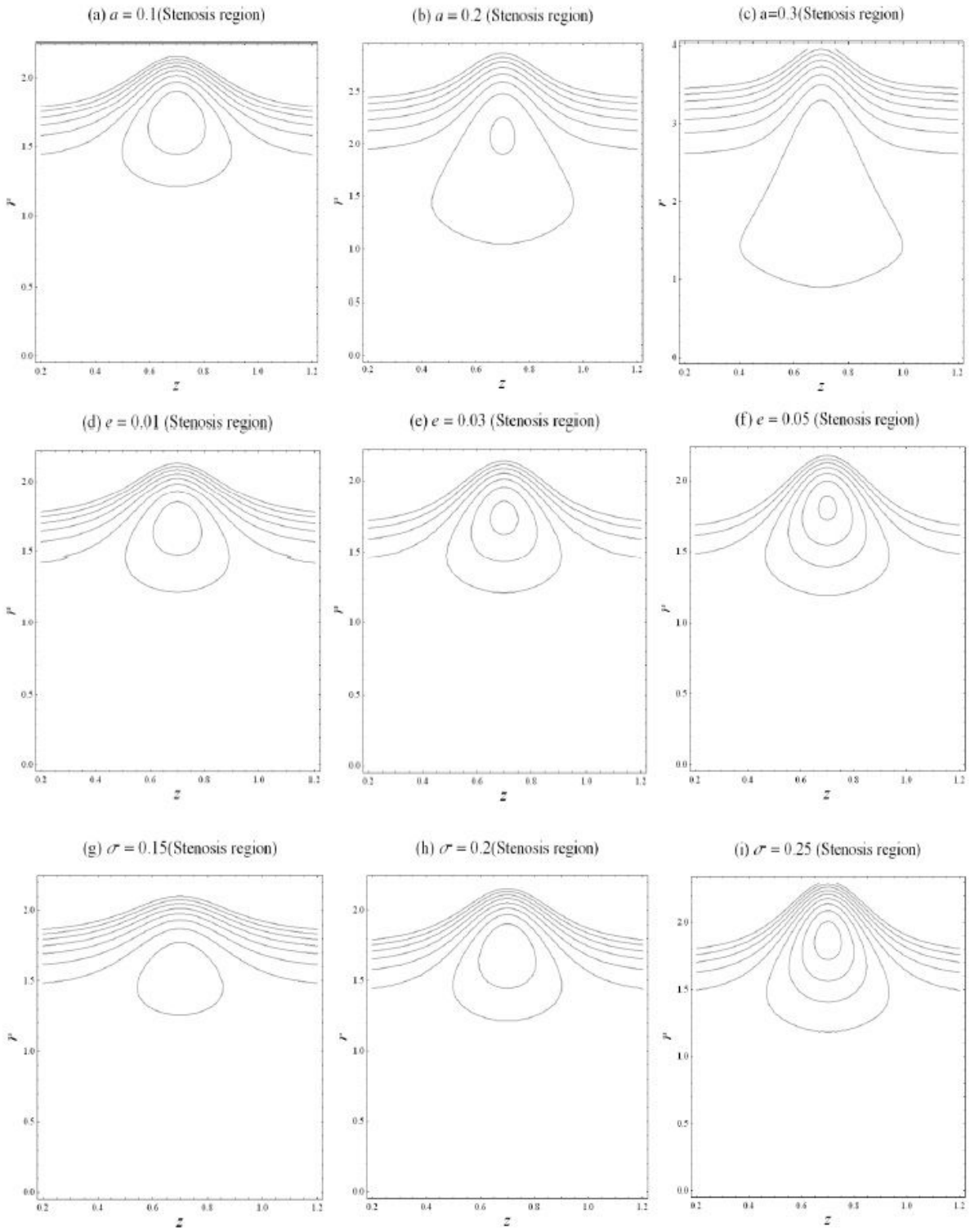

Figure 7

Streamlines with z in stenosis segment

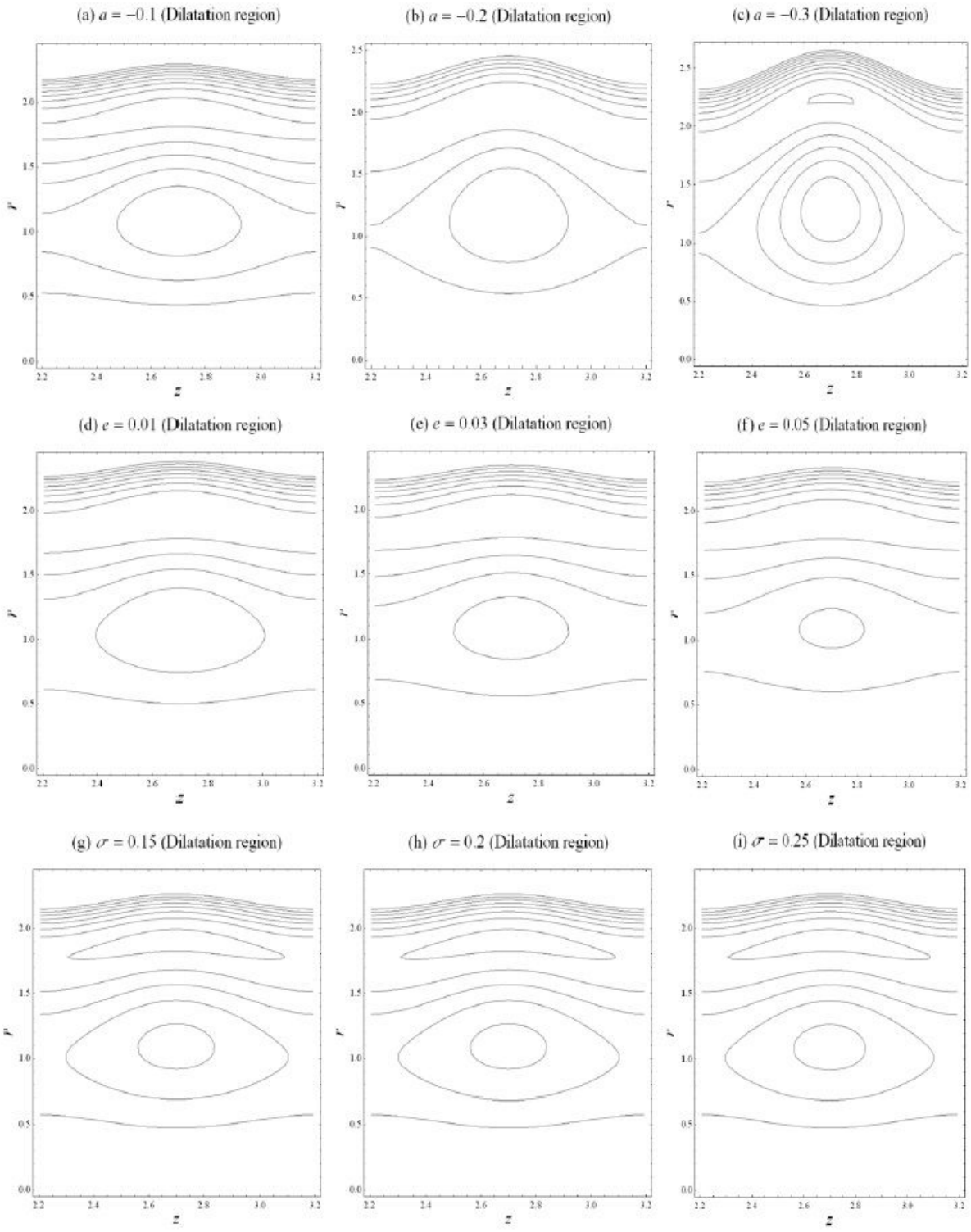

Figure 8

Streamlines with z in dilatation segment